British Journal of Pharmacology

British Journal of Pharmacology (2018) **175** 810–829 810

RESEARCH PAPER

Effects of corilagin on alleviating cholestasis via farnesoid X receptor-associated pathways *in vitro* and *in vivo*

Correspondence Professor Lei Zhao, Department of Infectious Diseases, Union Hospital, Tongji Medical College, Huazhong University of Science and Technology, Wuhan 430022, China. E-mail: leizhao@hust.edu.cn

Received 12 June 2017; **Revised** 22 November 2017; **Accepted** 24 November 2017

Fan Yang[1,*], Yao Wang[2,*], Gang Li[3,*], Juan Xue[4], Zhi-Lin Chen[5], Feng Jin[6], Lei Luo[7], Xuan Zhou[5], Qian Ma[8], Xin Cai[6], Hua-Rong Li[9] and Lei Zhao[5]

[1]Department of Hepatology, Hubei Provincial Hospital of Chinese Medicine, Wuhan, China, [2]Department of Infectious Diseases, Renmin Hospital of Wuhan University, Wuhan, China, [3]Department of Infectious Diseases, Renmin Hospital, Hubei University of Medicine, Shiyan, China, [4]Department of Gastroenterology, Hubei Province Hospital of Integrated Traditional Chinese and Western Medicine, Wuhan, China, [5]Department of Infectious Diseases, Union Hospital, Tongji Medical College, Huazhong University of Science and Technology, Wuhan, China, [6]Department of Neurosurgery, Affiliated Hospital of Jining Medical University and Shangdong Provincial Key Laboratory of Stem Cells and Neuro-oncology, Jining, Shandong, China, [7]School of First Clinical Medicine, Hubei University of Chinese Medicine, Wuhan, China, [8]School of Life Science, Hubei University, Wuhan, China, and [9]Department of Integrated Traditional Chinese and Western Medicine, Union Hospital, Tongji Medical College, Huazhong University of Science and Technology, Wuhan, China

*These authors contributed equally to this work.

BACKGROUND AND PURPOSE

The aim of this study was to investigate the ameliorative effects of corilagin on intrahepatic cholestasis induced by regulating liver farnesoid X receptor (FXR)-associated pathways *in vitro* and *in vivo*.

EXPERIMENTAL APPROACH

Cellular and animal models were treated with different concentrations of corilagin. In the cellular experiments, FXR expression was up-regulated by either lentiviral transduction or GW4064 treatment and down-regulated by either siRNA technology or treatment with guggulsterones. Real-time PCR and Western blotting were employed to detect the mRNA and protein levels of FXR, SHP1, SHP2, UGT2B4, BSEP, CYP7A1, CYP7B1, NTCP, MRP2 and SULT2A1. Immunohistochemistry was used to examine the expression of BSEP in liver tissues. Rat liver function and pathological changes in hepatic tissue were assessed using biochemical tests and haematoxylin and eosin staining.

RESULTS

Corilagin increased the mRNA and protein levels of FXR, SHP1, SHP2, UGT2B4, BSEP, MRP2 and SULT2A1, and decreased those of CYP7A1, CYP7B1 and NTCP. After either up- or down-regulating FXR using different methods, corilagin could still increase the mRNA and protein levels of FXR, SHP1, SHP2, UGT2B4, BSEP, MRP2 and SULT2A1 and decrease the protein levels of CYP7A1, CYP7B1 and NTCP, especially when administered at a high concentration. Corilagin also exerted a notable effect on the pathological manifestations of intrahepatic cholestasis, BSEP staining in liver tissues and liver function.

CONCLUSIONS AND IMPLICATIONS

Corilagin exerts a protective effect in hepatocytes and can prevent the deleterious activities of intrahepatic cholestasis by stimulating FXR-associated pathways.

DOI:10.1111/bph.14126

Abbreviations

ALP, alkaline phosphatase; ALT, alanine aminotransferase; ANIT, α-naphthylisothiocyanates; AST, aspartate aminotransferase; BA, bile acid; BSEP, bile salt export pump; CYP7A1, cytochrome P450 family 7 subfamily A polypeptide 1; CYP7B1, cytochrome P450 family 7 subfamily B polypeptide 1; DBIL, direct bilirubin; DEX, dexamethasone; FDA, Food and Drug Administration; FXR, farnesoid X receptor; HE, haematoxylin and eosin; IHC, immunohistochemistry; MRP2, multidrug resistance-associated protein 2; NTCP, sodium taurocholate cotransporting polypeptide; PBC, primary biliary cirrhosis; SHP1/2, small heterodimer partner 1/2; SULT2A1, sulfotransferase family 2A member 1; TU, transducing units; UDCA, ursodeoxycholic acid; UGT2B4, UDP glucuronosyltransferase 2 family polypeptide B4; γ-GGT, γ-glutamyl transpeptidase

Introduction

Intrahepatic cholestasis is an impairment of hepatocytes and cholangiocytes that can lead to bile formation and flow blockage, especially bile acid (BA) retention. Accordingly, biochemical indicators of this condition include elevated levels of total bilirubin (TBIL), direct bilirubin (DBIL), γ-glutamyl transpeptidase (γ-GGT), alkaline phosphatase (ALP) and total BAs (TBA) (Beuers *et al.,* 2015). If patients do not undergo effective treatment, they will develop liver fibrosis, cirrhosis and even liver failure, ultimately requiring liver transplantation (Ding *et al.,* 2006).

Ursodeoxycholic acid (UDCA) and glucocorticoids are recognized as effective drugs that are frequently used to treat cholestatic hepatitis (Parés, 2015). However, UDCA is ineffective in approximately 1/3 of patients with cholestasis, and the treatment is tedious (McKiernan, 2002), while glucocorticoids cause obvious side effects (Purohit and Cappell, 2015). Therefore, identifying drugs with fewer side effects with fast efficacy for treating cholestatic hepatitis is critical. During the progression of cholestasis, the nuclear receptor **farnesoid X receptor (FXR)** plays a central role in bile composition metabolism, which controls the balance of BAs by regulating their synthesis, detoxification and transport (Ding *et al.*, 2015a, b). Thus, FXR is considered a key target for the treatment of cholestasis (Sepe *et al.,* 2015).

Corilagin (β-1-O-galloyl-3,6-(R)-hexahydroxydiphenoyl-D-glucose), which is found in many medicinal herbaceous plants such as *Phyllanthus urinaria*, is a member of the tannin family (Shen *et al.,* 2003). Its molecular formula is $C_{27}H_{22}O_{18}$ (Duan *et al.,* 2005). Corilagin has been found to have strong antioxidant (Zhao *et al.,* 2008; Jin *et al.,* 2013), anti-inflammatory (Zhao *et al.,* 2008), hepatoprotective (Shiota *et al.,* 2004), thrombolytic and antihypertensive (Cheng *et al.,* 1995), antiatherogenic (Duan *et al.,* 2005) and antitumoural (Jia *et al.,* 2013) properties. Corilagin can also suppress schistosomiasis liver fibrosis by regulating the IL-13/JAK/STAT6 and miR-21/smad7/ERK signalling pathways (Li *et al.,* 2016; Yang *et al.,* 2016; Du *et al.,* 2016). Moreover, corilagin inhibits the expression of TNF-α and NF-κB (Gambari *et al.,* 2012) and protects against HSV1 encephalitis by inhibiting the TLR2 signalling pathways (Guo *et al.,* 2015; Guo *et al.,* 2010).

In our previous study, we demonstrated that corilagin exerts anti-inflammatory and anti-oxidative effects against acute cholestasis (Jin *et al.,* 2013). However, the molecular mechanism through which corilagin alleviates intrahepatic cholestasis is still unknown. As α-naphthylisothiocyanate (ANIT) treatment results in pathological and biochemical changes in the liver that mimic those of cholestatic hepatitis (Chen *et al.,* 2016; Ding *et al.,* 2008), in this study we used the normal liver tissue LO2 cell line and an ANIT-induced rat model of cholestasis to determine whether corilagin can alleviate cholestasis via the FXR-associated signalling pathway and to find a new strategy to prevent and treat intrahepatic cholestasis.

Methods

Cell culture and cytotoxic effects of corilagin

The LO2 human embryo liver cell line was purchased from the Chinese Academy of Sciences. RPMI 1640 medium supplemented with 10% FBS was used to culture the LO2 cells in an incubator at 37°C and maintained in a humidified atmosphere containing 5% CO_2. The cytotoxic effect of corilagin was evaluated by assessing cell numbers using a cell counting kit (CCK8 assay), which was conducted as previously described (Wang *et al.,* 2016).

FXR in cells up- or down-regulated with GW4064 or guggulsterones

The treatment groups were divided into a normal group, a **dexamethasone** (DEX)- treated group, a UDCA group and corilagin 25, 50 and 100 $\mu g \cdot mL^{-1}$ groups. LO2 cells were maintained in RPMI 1640 media supplemented with 10% FBS. As previously described (Ding *et al.,* 2016), cells were distributed into either six-well plates for real-time PCR and Western blotting or 96-well plates for the CCK8 experiments and preliminary lentiviral transfection experiments for 24 h. When the cell cultures reached 70% density, they were treated with corilagin, UDCA or DEX. After 24 h, the cells were harvested for real-time PCR and Western blotting. For the experiments involving treatment with **GW4064** or **guggulsterones**, LO2 cells were maintained in RPMI 1640 media supplemented with 10% FBS. After the cells were grown on six-well plates for 24 h and cultured to 70% density, GW4064 (1 $\mu mol \cdot L^{-1}$, diluted in 1640 medium) or guggulsterones (1 $\mu mol \cdot L^{-1}$, diluted in 1640 medium) were added to the wells of all the groups (except the normal group) for 24 h. Then, the cells were treated with corilagin, UDCA or DEX, as indicated above. After 24 h, the cells were harvested for real-time PCR and Western blotting.

Small interfering RNA (siRNA) transfection of LO2 cells

Human FXR siRNA (sense 5′-CAAGTGACCTCGACAACAA-3′) was synthesized by RiboBio Co., Ltd., GenePharma Co. Ltd.

(Guangzhou, China). LO2 cells were seeded onto six-well plates and transfected with 50 μmol·mL^{-1} siRNA constructs using 20 pmol·mL^{-1} Lipofectamine 2000 (Invitrogen, San Diego, USA) according to the manufacturer's instructions. The medium was replaced 6 h later, and then, the cells were cultured for up to 48 h. In addition, the siRNA-transfected cells were treated with corilagin, UDCA or DEX 24 h before harvesting.

Overexpression of FXR in LO2 cells via lentiviral transduction

The FXR and control lentiviral vectors were constructed by GeneChem Co., Ltd. (Shanghai, China). GV367-FXR/NC-eGFP was transfected into LO2 cells, and the viral supernatant was harvested after 48 h (2×10^8 transducing units·mL^{-1}). LO2 cells were seeded onto 96-well or 6-well plates and transduced with lentivirus with a multiplicity of infection of 50 according to the manufacturer's instructions. The medium was replaced 6 h later, and then, the cells were grown for an additional 72 h. In addition, the lentivirus-transfected cells were treated with corilagin, UDCA or DEX for another 24 h.

Animals

Neonatal Sprague–Dawley male rats (3 weeks old) weighing 40–50 g and rats for isolating primary hepatocytes were born and raised in specific pathogen-free conditions and were purchased from Hubei Provincial Centre for Disease Control and Prevention (Wuhan, China). Animal studies are reported in compliance with the ARRIVE guidelines (Kilkenny *et al.*, 2010; McGrath and Lilley, 2015). Rats were housed in stainless polypropylene cages (size: 465 x 290 x 150 mm) with wood shavings as bedding materials. A maximum of five rats was kept in a single cage. The rats were maintained as described previously (Du *et al.*, 2016) under standard laboratory conditions at 25 ± 2°C, 50 ± 15% relative humidity and a normal circadian period (12 h dark/12 h light cycle). The animals were provided a normal diet and water *ad libitum*. All study procedures were approved by internationally accepted principles and the Guidelines for the Care and Use of Laboratory Animals of Huazhong University of Science and Technology.

Rat model establishment and drug administration

Thirty-five rats were equally divided into seven groups: corilagin (40 mg·kg^{-1}), corilagin (20 mg·kg^{-1}), corilagin (10 mg·kg^{-1}), UDCA, model and normal (rats not treated with ANIT). The LD_{50} of corilagin is 1.78 g·kg^{-1} (Zhang *et al.*, 2013), which is much larger than our experimental dose. Corilagin was prepared as a 0.4% suspension in sodium carboxymethylcellulose. UDCA was prepared as a 0.6% suspension in water. Dexamethasone was dissolved in water at a concentration of 0.045%. Our previous studies confirmed that liver damage and pathological changes began to increase 24 h after ANIT treatment, peaked at 48 h and tended to be absent at 72 h (Ding *et al.*, 2008). ANIT was dissolved in sesame oil at a concentration of 1% and administered for 48 h. Before establishing the cholestasis model, corilagin (40 mg·kg^{-1}), corilagin (20 mg·kg^{-1}), corilagin (10 mg·kg^{-1}), UDCA (60 mg·kg^{-1}·day^{-1}) and DEX (1.8 mg·kg^{-1}·day^{-1}) were intragastrically administered to the rats in their respective groups for 4 days. Model and normal groups were administered normal saline. On the fifth day, we induced the rat model of cholestasis. In addition, after 12 h, all the groups (except the normal group) were intragastrically administered ANIT (50 mg·kg^{-1}). Eight hours after administration of ANIT, the rats were administered the respective drug or control agents. After 48 h of continuous ANIT treatment, the rats in each group were killed to collect specimens (Table 1 and Figure 9A). Rats were assigned to groups randomly, and no rats were excluded from the statistical analysis.

Specimen collection

The procedure was conducted as previously described (Yang *et al.*, 2016). Rats were anaesthetized with 4% chloral hydrate (1 mL·100 g^{-1}, i.p.), the abdomen was opened, and the abdominal aorta was separated. Then, 2–3 mL of arterial blood was collected in a test tube containing anticoagulant. After centrifugation at 3250 *g*, blood serum was obtained and stored at −20°C until testing. Subsequently, the rat liver was dissected using an aseptic, RNase-free device. After washing with normal saline, the entire hepatic tissue was divided into two parts – one part was sheared and stored at −80°C, and the other was fixed in 10% formalin for 48 h, dehydrated and embedded in paraffin and sliced.

Isolation, culture and treatment of rat primary hepatocytes

Hepatocytes from male SD rats (8–9 weeks) weighing 200–220 g were isolated by a two-step collagenase digestion method and cultured according to published procedures (Klaunig *et al.*, 1981; Chen *et al.*, 2014). CK-18 protein in

Table 1

The dosage of medication and time of administration in the animal experiments

Dosage of medication
High dose of corilagin: 40 mg·kg^{-1}·day^{-1}
Middle dose of corilagin: 20 mg·kg^{-1}·day^{-1}
Low dose of corilagin: 10 mg·kg^{-1}·day^{-1}
DEX: 1.8 mg·kg^{-1}·day^{-1}
UDCA: 60 mg·kg^{-1}·day^{-1}
ANIT: 50 mg·kg^{-1}
Time of administration
Day 1 to Day 5: corilagin, DEX and UDCA administered each day for 4 days
Day 5: 12 h after the administration of corilagin, DEX or UDCA administration, ANIT was injected i.g. to induce a rat model of choleostasis (we defined this modelling time point as time point A.)
8 h after time point A: corilagin, DEX or UDCA was administered.
48 h after time point A: specimen collected.

the cells was detected by immunofluorescence to identify whether the isolated cells were rat primary hepatocytes (Banaudha *et al.,* 2010). Then, the hepatocytes were seeded in six-well plates. When the cell cultures reached 70% density, they were treated with corilagin, UDCA or DEX. After 24 h, the cells were harvested for real-time PCR and Western blotting.

Biochemical tests

The serum alanine aminotransferase (ALT), aspartate aminotransferase (AST), TBIL, DBIL, ALP, γ-GGT and TBA levels were assayed using a fully automated Aeroset Chemistry Analyser provided by Abbott Co., Ltd. (Ding *et al*., 2008).

Real-time quantitative PCR

Following our previous protocols (Huang *et al.,* 2013; Zhou *et al.,* 2016), total RNA from liver tissues and cells was isolated using RNAiso Plus following the manufacturer's instructions. cDNAs were produced using a PrimeScript RT reagent kit and incubated at 37°C for 15 min and 85°C for 5 s. Real-time PCR reactions were performed using a StepOne Plus device (Applied Biosystems) at 95°C for 10 s followed by 40 cycles of 95°C for 5 s and 60°C for 20 s according to the instructions provided by the SYBR Premix Ex Taq kit. Data were analysed using the $2^{-\Delta\Delta Ct}$ method (Schmittgen and Livak, 2008). All primers were synthesized by TSINGKE (Wuhan, China). The sequences of all primers are listed in Table 2.

Western blot analysis

Western blotting was performed as previously described (Zhao *et al.,* 2008). To detect FXR, **SHP1**, SHP2, **BSEP (ABCB11; ABC16)** and UGT2B4 expression, total protein was extracted from the liver tissues and hepatocytes. Protein concentration was determined using the bicinchoninic acid method. In each sample, an equivalent volume of 2× SDS loading buffer (100 mM Tris–HCl, pH 6.8; 4% SDS; 20% glycerine; 10% β-mercaptoethanol; and 0.2% bromophenol blue) was added and mixed again. The mixtures were then denatured at 95°C for 10 min, and approximately 30 mg of protein was loaded into each well and separated on 10% SDS-PAGE gels. After separation for approximately 80 min, the proteins were transferred to PVDF membranes, and the membranes were saturated and blocked with 5% fat-free milk at 37°C for 1 h. The membranes were probed with rabbit polyclonal antibodies targeting the rat homologues of FXR (1:1000), BSEP (1:1000), UGT2B4 (1:500), SHP1 (1:1000), SHP2 (1:1000), **CYP7A1** (1:1000), **CYP8B1** (1:1000), **NTCP (SLC10A1**; 1:1000), **MRP2 (ABCC2;** 1:1000), SULT2A1 (1:2000) and β-actin (1:5000) followed by treatment with HRP-conjugated secondary immunoglobulin IgG (1:1000). The membranes were then treated with an enhanced chemiluminescence reagent (Merck Millipore, MA, USA), and the signals were detected by exposing the membranes to X-ray films (Kodak, Rochester, NY, USA). The relative signal intensity was quantified using densitometry with Gel pro3.0 image software (Media Cybernetics, Silver Spring, MD, USA) on an IBM-compatible personal computer.

Immunohistochemistry (IHC) for detecting BSEP expression in liver tissue

IHC was conducted as previously described (Jin *et al.,* 2015). The liver tissue specimens were sliced into 10 μm sections after dewaxing and rehydrating. The sections were incubated in 3% H_2O_2/methanol to eliminate endogenous peroxidase activity. Then, the sections were incubated with normal goat serum for 10 min followed by BSEP antibody (1:400) overnight at 4°C and biotin-conjugated goat anti-rabbit IgG (1:500) at 37°C for 45 min. The sections were rinsed again with PBS and incubated with HRP-conjugated streptavidin at 37°C. The samples were developed with diaminobenzidine and stained with haematoxylin. After being rinsed with distilled water and dehydrated, the sections were made transparent and mounted for examination under a microscope. After immunohistochemical analysis, Image-Pro plus software version 6.0 was used to analyse the optical density of the images as described previously.

Histomorphology

After the tissues were fixed in 4% formaldehyde, they were embedded in paraffin and cut into 4-mm-thick serial sections

Table 2

Sequences of primers for real-time quantitative

Gene	Primer sequence	Human(5′ → 3′)	Rat(5′ → 3′)
FXR	Forward primer	5′-AAGTGACCTCCACGACCAAGC-3′	5′-AAGAGATGGGAATGTTGGCTG-3′
	Reverse primer	5′-TCCGCTGAACGAAGGAACAT-3′	5′-CTCCCTGCATGACTTTGTTGTC-3′
SHP	Forward primer	5′-GAAAGGCACTATCCTCTTCAACC-3′	5′-GAAAGGGACCATCCTCTTCAAC-3′
	Reverse primer	5′-AGATGTTCTTGAGGGTGGAAGC-3′	5′-TCTCCAATGATAGGGCGAAAG-3′
BSEP	Forward primer	5′-ATGTTGACGGGATTCGCTTC-3′	5′-CAACTGCTGGACCGACAACC-3′
	Reverse primer	5′-CCACTCCAATCCCAGCAACT-3′	5′-CATCCACTGCTCCCAACAAAC-3′
UGT2B4	Forward primer	5′-CACTGCAAACCTGCTAAACCC-3′	5′-GGTCGATGGTCAGTAACACGTC-3′
	Reverse primer	5′-GTATTGGGTCCTAAGGTGGGTG-3′	5′-TTGTACAGCCGAGTATTGAGTCCT-3′
β-actin	Forward primer	5′-CGTTGACATCCGTAAAGACCTC-3′	5′-GTCCACCGCAAATGCTTCTA-3′
	Reverse primer	5′-TAGGAGCCAGGGCAGTAATCT-3′	5′-TGCTGTCACCTTCACCGTTC-3′

for haematoxylin and eosin (HE) staining as described previously (Huang *et al.,* 2013).

Statistical analysis

The statistical analyses were conducted using SPSS 12.0 software. Data are expressed as the mean ± SD. The significance of differences between two groups was determined by Student's paired two-tailed *t*-test. For all other statistical analyses and comparisons of multiple groups one-way ANOVA was used followed by Tukey's *post hoc* test. Statistical significance was defined as $P < 0.05$ (Ding *et al.*, 2015a, b; Dang *et al.,* 2016). The data and statistical analysis complied with the recommendations on experimental design and analysis in pharmacology (Curtis *et al.*, 2015).

Chemicals and reagents

Corilagin (purity >99%) for cell experiments was purchased from the China National Institutes for Food and Drug Control. Corilagin for animal experiments (purity >80%), which was used in our previous study (Yang *et al.,* 2016), was provided by Chengdu PureChem-Standard Co., Ltd. (Chengdu, China). A Cell Counting Kit 8 (CCK8) kit was purchased from Dojindo Laboratories (Kumamoto, Japan). ANIT was purchased from Sigma (St Louis, MO, USA). UDCA capsules were obtained from Dr Falk at Pharma GmbH (Freiburg, Germany). Dexamethasone (DEX) was purchased from Xinxiang Changle Pharmaceutical Company Ltd. (Xinxiang, China). Guggulsterones and GW4064 were purchased from Santa Cruz Biotechnology (Santa Cruz, CA, USA). FBS and RPMI 1640 medium were obtained from Gibco (Grand Island, NY, USA). Protein extraction kits were purchased from Wuhan Aspen Biological Technology co., Ltd. (Wuhan, China). Affinity-purified rabbit anti-rat antibodies targeting bile salt export pump (BSEP), UGT2B4, **SHP**1, SHP2, CYP7A1, CYP8B1, NTCP, **MRP2**, **SULT2A1** and cytokeratin-18 (CK-18) were purchased from Abcam (Cambridge, MA, USA). Rabbit anti-rat intercellular FXR was obtained from Cell Signaling Technology Inc. (Beverly, MA, USA). Biotin-conjugated goat anti-rabbit IgG and streptavidin-HRP conjugate were obtained from Wuhan Boster Biotechnology Co., Ltd. (Wuhan, China). RNAiso, a PrimeScript RT Reagent kit and a SYBR Premix Ex Taq kit were obtained from Takara Biotechnology Dalian Co., Ltd. (Dalian, China).

Nomenclature of targets and ligands

Key protein targets and ligands in this article are hyperlinked to corresponding entries in http://www.guidetopharmacology.org, the common portal for data from the IUPHAR/BPS Guide to PHARMACOLOGY (Southan *et al.*, 2016), and are permanently archived in the Concise Guide to PHARMACOLOGY 2017/18 (Alexander *et al.,* 2017a,b,c).

Results

Cytotoxic effect of corilagin and cell morphology observation

Cell viability (%) was calculated as follows: [A (experimental well) − A (blank well)] / [A (control well) − A (blank well)] × 100. Moreover, we assessed the viability of cells treated with different concentrations (0, 6.25, 12.5, 25, 50, 100, 200 and 400 $\mu g \cdot mL^{-1}$) of corilagin after 24 h. Based on the CCK8 assay, the concentration–effect curve was represented by the equation y = 100/(1 + 10^((2.228-x)*(−2.210))) (Figure 1A), and the specific parameters IC_{50} (169.0 $\mu g \cdot mL^{-1}$), Hill slope (−2.210) and R^2 (0.9777) were also assessed. Then, using this equation, the concentration for 75% viability was calculated as 102.8272 $\mu g \cdot mL^{-1}$. For convenience, we approximated the highest concentration to 100 $\mu g \cdot mL^{-1}$, middle concentration as 50 $\mu g \cdot mL^{-1}$ and low concentration as 25 $\mu g \cdot mL^{-1}$. Thus, the concentrations of corilagin for pretreatment of unstimulated LO2 cells were 25, 50 and 100 $\mu g \cdot mL^{-1}$ for 24 h, none of which significantly affected cell viability (Figure 1B). Cell morphology observations showed the same result (Figure 1C, D). Therefore, we chose to treat cells with corilagin at 25, 50 and 100 $\mu g \cdot mL^{-1}$ for 24 h. We suggest that the IC_{50} of corilagin for LO2 cells is 169.0 $\mu g \cdot mL^{-1}$.

Effects of corilagin on the FXR and downstream effectors in LO2 cells

BAs are synthesized from cholesterol in hepatocytes, and hepatocytes play an important role in the entire process of BA metabolism. Therefore, we administered the three concentrations of corilagin selected to normal LO2 cells and observed whether corilagin could activate the FXR pathway. Compared with the untreated cells, the corilagin-treated cells showed significantly elevated mRNA expression of FXR, SHP, UGT2B4 and BSEP. The mRNA expression of FXR in the DEX group and the mRNA expression of SHP, UGT2B4 and BSEP in the UDCA group were also increased. More importantly, the increases in the mRNA levels of FXR, SHP, UGT2B4 and BSEP in the 100 $\mu g \cdot mL^{-1}$ corilagin group were greater than those in the DEX and UDCA groups (Figure 2A). The protein expression levels of FXR, SHP1, SHP2, UGT2B4, BSEP, MRP2 and SULT2A1 were also significantly increased. Furthermore, CYP7A1, CYP8B1 and NTCP were decreased in the corilagin groups compared with the normal group, and there were no obvious increases in protein expression in the DEX and UDCA groups (Figure 2B, C).

Effects of corilagin on FXR and downstream effectors in LO2 cells stimulated with guggulsterones

To identify the role of FXR in cholestasis, various researchers have sought to use chemicals or genetic tools to inhibit hepatic FXR. Some reports showed that Fxr-knockout (Fxr−/−) mice had excessive levels of BAs, cholesterol and triglycerides (Anakk *et al.,* 2011). Guggulsterones, which are FXR antagonists, have been proven to exacerbate cholestasis in liver cells (Zhao *et al.,* 2014). Therefore, in our experiment, LO2 cells were treated with guggulsterones to down-regulate FXR. Compared with the normal group, the guggulsterones group showed significantly decreased mRNA expression of FXR, SHP, UGT2B4 and BSEP, while compared with the guggulsterones group, the corilagin and UDCA groups showed significantly elevated mRNA expression of FXR, SHP, UGT2B4 and BSEP. The FXR and SHP mRNA levels in the 50 $\mu g \cdot mL^{-1}$ corilagin group and the FXR, SHP, UGT2B4 and BSEP mRNA levels in the 100 $\mu g \cdot mL^{-1}$ corilagin group were greater than

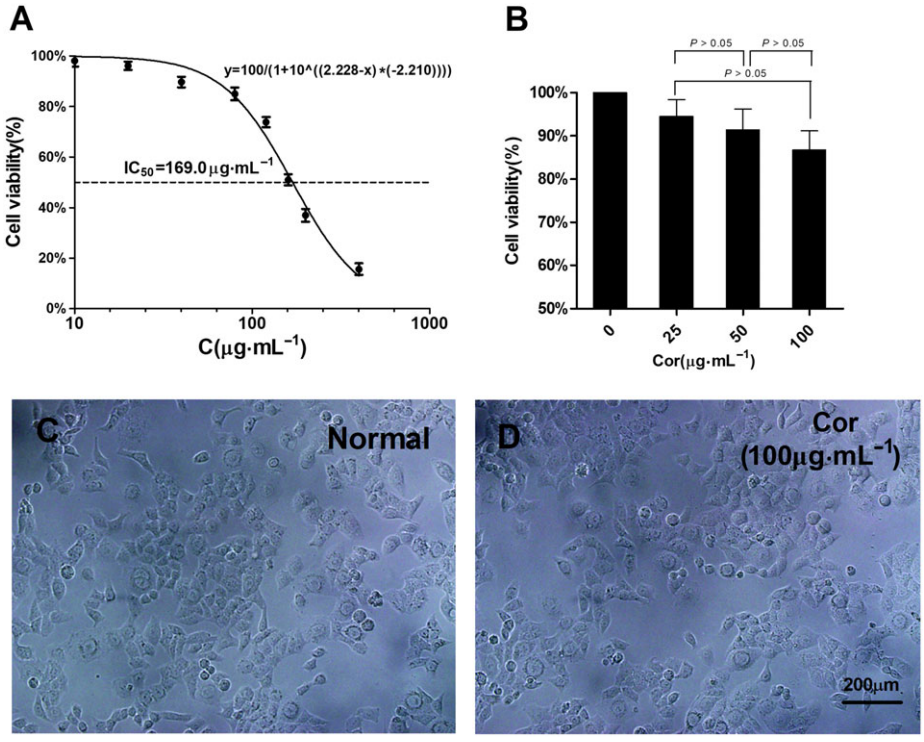

Figure 1

(A) The concentration–effect curve for corilagin (C) on LO2 cells was y = 100/(1 + 10^((2.228-x)*(−2.210))). IC_{50}: 169.0 μg·mL^{-1}; Hill slope: −2.210; R^2: 0.9777. (B) CCK8 assay of LO2 cell viability after corilagin (Cor) treatment. (C, D) Morphologies of LO2 after corilagin treatment for 24 h. Data are shown as the mean ± SD. n = 5.

those in the UDCA group (Figure 3A). The protein expression levels of FXR, SHP1, SHP2, UGT2B4, BSEP, MRP2 and SULT2A1 were also significantly reduced, while CYP7A1, CYP8B1 and NTCP were elevated by guggulsterones. The corilagin groups exhibited significantly higher protein expression of FXR, SHP1, SHP2, UGT2B4, BSEP, MRP2 and SULT2A1 and decreased protein expression of CYP7A1, CYP8B1 and NTCP than the guggulsterones group. It was worth noting that the activating effect on FXR protein increased as the concentration of corilagin increased (Figure 3B, C).

Effects of corilagin on FXR and downstream molecules in LO2 cells stimulated with GW4064

Either the FXR agonist 6α-ethyl-chenodeoxycholic acid (obeticholic acid) or GW4064 can reduce oestradiol-induced cholestasis in liver cells (Seok *et al.*, 2014) to increase the uptake of bile salts, restore the flow of bile and reduce the levels of serum bile salt. These compounds have been approved for the treatment of primary biliary cirrhosis (PBC) and NASH (Neuschwander-Tetri *et al.*, 2015). More importantly, to determine whether corilagin could continue to promote the FXR signalling pathway in the condition of high FXR levels, we used GW4064 to up-regulate FXR. Compared with the normal group, the GW4064 group showed significantly increased mRNA expression of FXR, SHP, UGT2B4 and BSEP, while compared with the GW4064 group, the 50 and 100 μg·mL^{-1} corilagin groups showed significantly increased mRNA expression of FXR, SHP, UGT2B4 and BSEP (Figure 4A). FXR, SHP1, SHP2, UGT2B4, BSEP, MRP2 and SULT2A1 protein expression was also significantly elevated and CYP7A1, CYP8B1 and NTCP protein expression was reduced in the GW4064 group. Compared with the GW4064 group, the corilagin and UDCA groups exhibited significantly elevated protein expression levels of FXR, SHP1, SHP2, UGT2B4, BSEP, MRP2 and SULT2A1, together with reduced protein expression levels of CYP7A1, CYP8B1 and NTCP. The BSEP protein levels in the 100 μg·mL^{-1} corilagin group were significantly higher than those in the UDCA group (Figure 4B, C).

Effect of corilagin on FXR and downstream effectors in LO2 cells after siRNA down-regulation of FXR

To selectively down-regulate the expression of FXR, we used siRNA to interfere with FXR in LO2 cells. In addition, to verify whether the FXR-siRNA was transfected into the cells, the Cy3 molecule in LO2 cells was conjugated to the siRNA and observed under a fluorescence microscope after siRNA transfection for 24 h (Figure 5A–C). The cells were then treated with corilagin (25, 50 or 100 μg·mL^{-1}), UDCA or DEX for 24 h. Compared with the normal group, the Si-FXR group showed significantly decreased mRNA expression levels of FXR, SHP, UGT2B4 and BSEP (Figure 5D), and the protein expression levels of FXR, SHP1, SHP2, UGT2B4, BSEP, MRP2

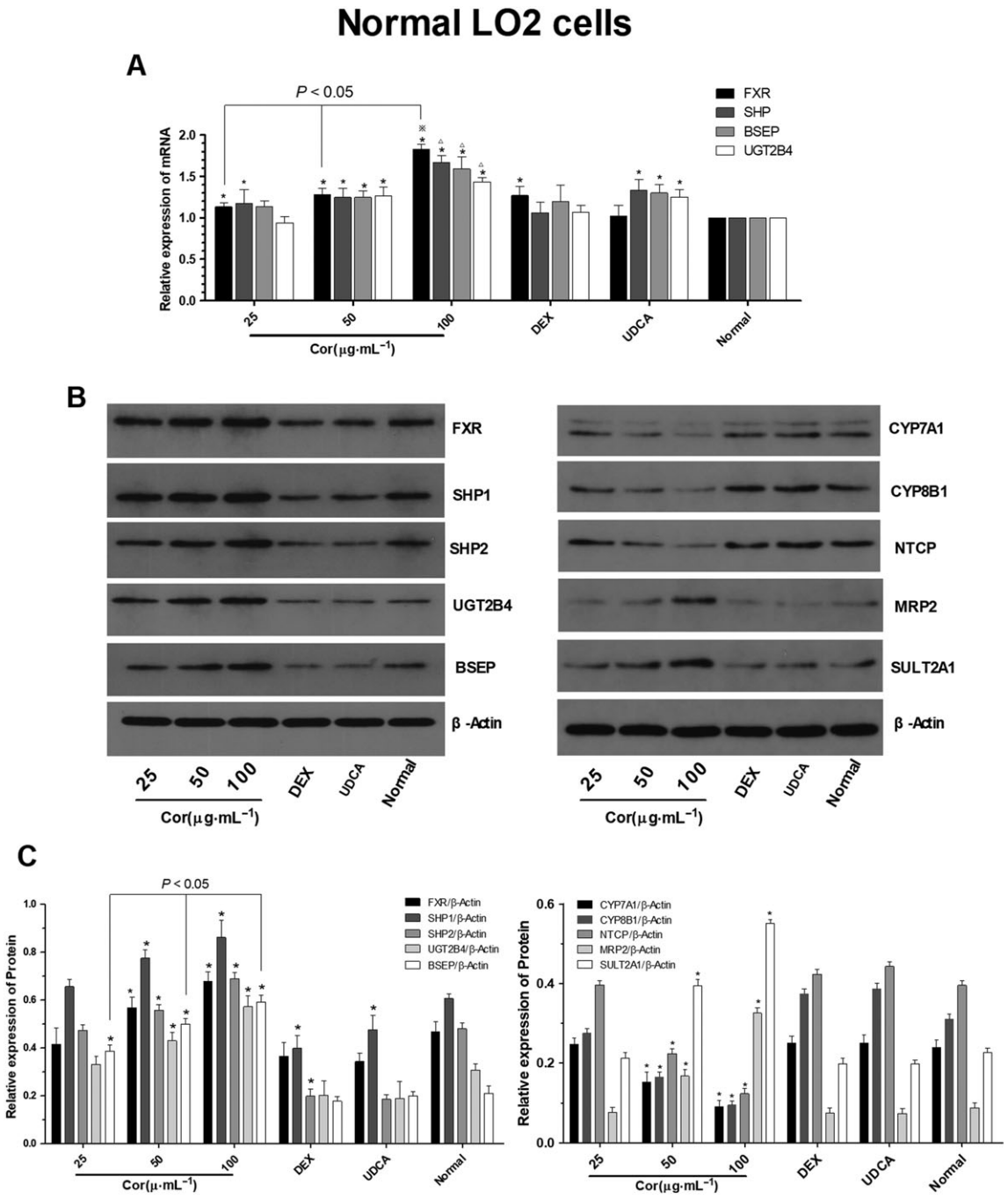

Figure 2

Effect of corilagin on the expression of FXR, SHP, BSEP and UGT2B4 in LO2 normal cells. (A) The mRNA levels of FXR SHP, BSEP and UGT2B4 were detected by RT-PCR. (B, C) The protein levels of FXR, SHP1, SHP2, BSEP, UGT2B4, MRP2, SULT2A1, CYP7A1, CYP8B1 and NTCP were detected by Western blotting. Data are shown as the mean ± SD. $n = 5$. (*$P < 0.05$ compared to the Normal group).

and SULT2A1 were also significantly lower, while CYP7A1, CYP8B1 and NTCP were higher in the Si-FXR group (Figure 5E–G). Compared with the Si-FXR group, the corilagin and UDCA groups exhibited significantly elevated mRNA expression levels of FXR, SHP, UGT2B4 and BSEP. In addition, the FXR mRNA levels in the 50 and 100 μg·mL^{-1} corilagin groups and the SHP, UGT2B4 and BSEP mRNA levels in 100 μg·mL^{-1} corilagin group were notably more elevated than those in the UDCA group. The activating effect of FXR mRNA increased as the concentration of corilagin increased (Figure 5H). Compared with the Si-FXR group, the corilagin and UDCA groups showed significantly elevated protein expression levels of FXR, SHP1, SHP2, UGT2B4, BSEP, MRP2 and SULT2A1, as well as significantly reduced protein

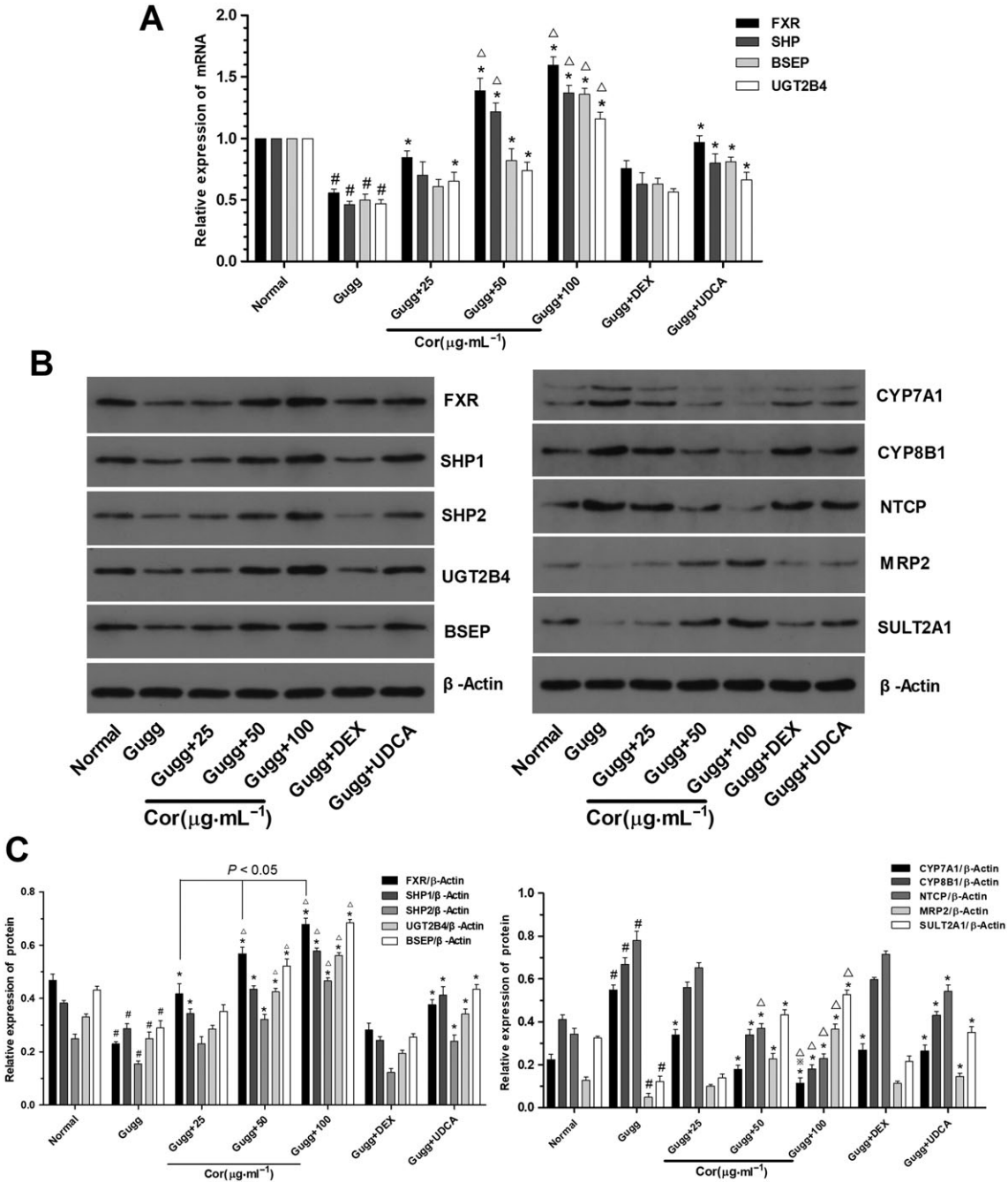

Figure 3

Effect of corilagin on the expression of FXR, SHP, BSEP, UGT2B4, MRP2, SULT2A1, CYP7A1 and CYP8B1 in the guggulsterones (Gugg)-treated LO2 cells. (A) The mRNA levels of FXR SHP, BSEP and UGT2B4 were detected by RT-PCR. (B, C) The protein levels of FXR, SHP1, SHP2, BSEP, UGT2B4, MRP2, SULT2A1, CYP7A1, CYP8B1 and NTCP were detected by Western blotting. Data are shown as the mean ± SD. $n = 5$. (*$P < 0.0$ compared to the Gugg group; #$P < 0.05$ compared to the Normal group; △$P < 0.05$ compared to the UDCA group).

expression levels of CYP7A1, CYP8B1 and NTCP. In addition, the SHP1 protein levels in the 50 and 100 μg·mL^{-1} corilagin groups and the FXR, SHP2, UGT2B4, MRP2, SULT2A1, CYP7A1, CYP8B1 and NTCP protein levels in the 100 μg·mL^{-1} corilagin group were notably more elevated than those in the UDCA group (Figure 5I–L).

Effect of corilagin on downstream effectors in LO2 cells after up-regulation of FXR using a lentiviral vector

To selectively down-regulate the expression of FXR, we constructed the FXR lentiviral vector GV273 and transduced LO2 cells *in vitro*. Green fluorescent protein (GFP) was

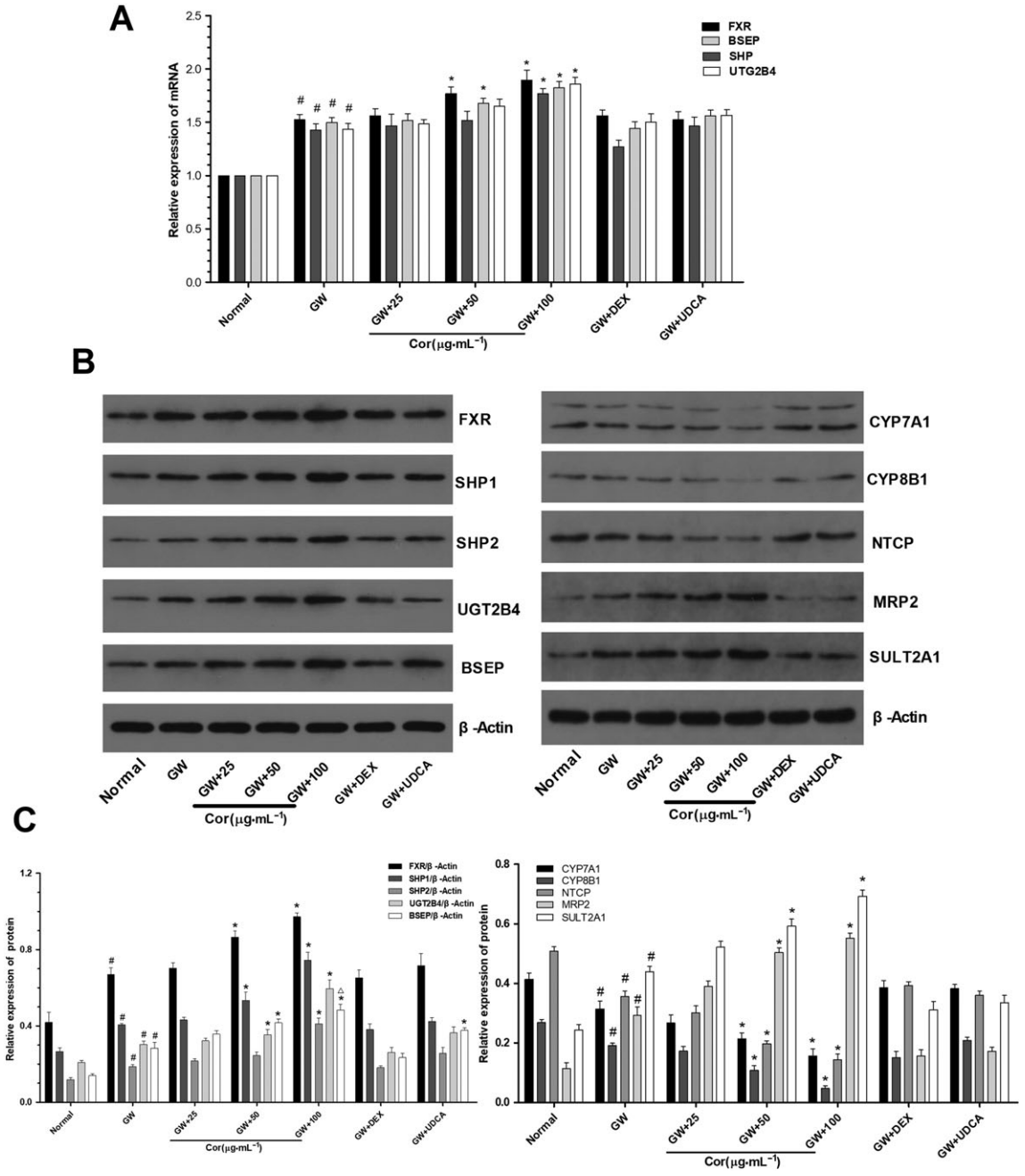

Figure 4

Effect of corilagin on the expression of FXR, SHP, BSEP, UGT2B4, MRP2, SULT2A1, CYP7A1 and CYP8B1 in the GW4064 (GW)-treated LO2 cells. (A) The mRNA levels of FXR SHP, BSEP and UGT2B4 were detected by RT-PCR. (B, C) The protein levels of FXR, SHP1, SHP2, BSEP, UGT2B4, MRP2, SULT2A1, NTCP, CYP7A1 and CYP8B1 were detected by Western blotting. Data are shown as the mean ± SD. $n = 5$. (*$P < 0.05$ compared to the GW group; #$P < 0.05$ compared to the Normal group; △$P < 0.05$ compared to the UDCA group).

observed under a fluorescence microscope at 48 and 72 h after transduction (Figure 6A, B). Then, the cells were treated with corilagin (25, 50 or 100 μg·mL^{-1}), UDCA or DEX for 24 h. Compared with the normal group, the lentivirus-treated group showed significantly increased mRNA expression levels of FXR, SHP, UGT2B4 and BSEP (n = 5; $P < 0.05$) (Figure 6C), and the protein expression levels of FXR, SHP1, SHP2, UGT2B4, BSEP, MRP2 and SULT2A1 were also significantly elevated, while CYP7A1, CYP8B1 and NTCP were reduced in the lentivirus-treated group (Figure 6D–F). The corilagin and UDCA groups exhibited significantly higher mRNA expression levels of FXR, SHP, UGT2B4 and BSEP than the lentivirus-treated group. In addition, the FXR and BSEP mRNA levels in the 100 μg·mL^{-1} corilagin groups were more pronounced than those in the UDCA group (Figure 6G). Compared with the lentivirus-treated group,

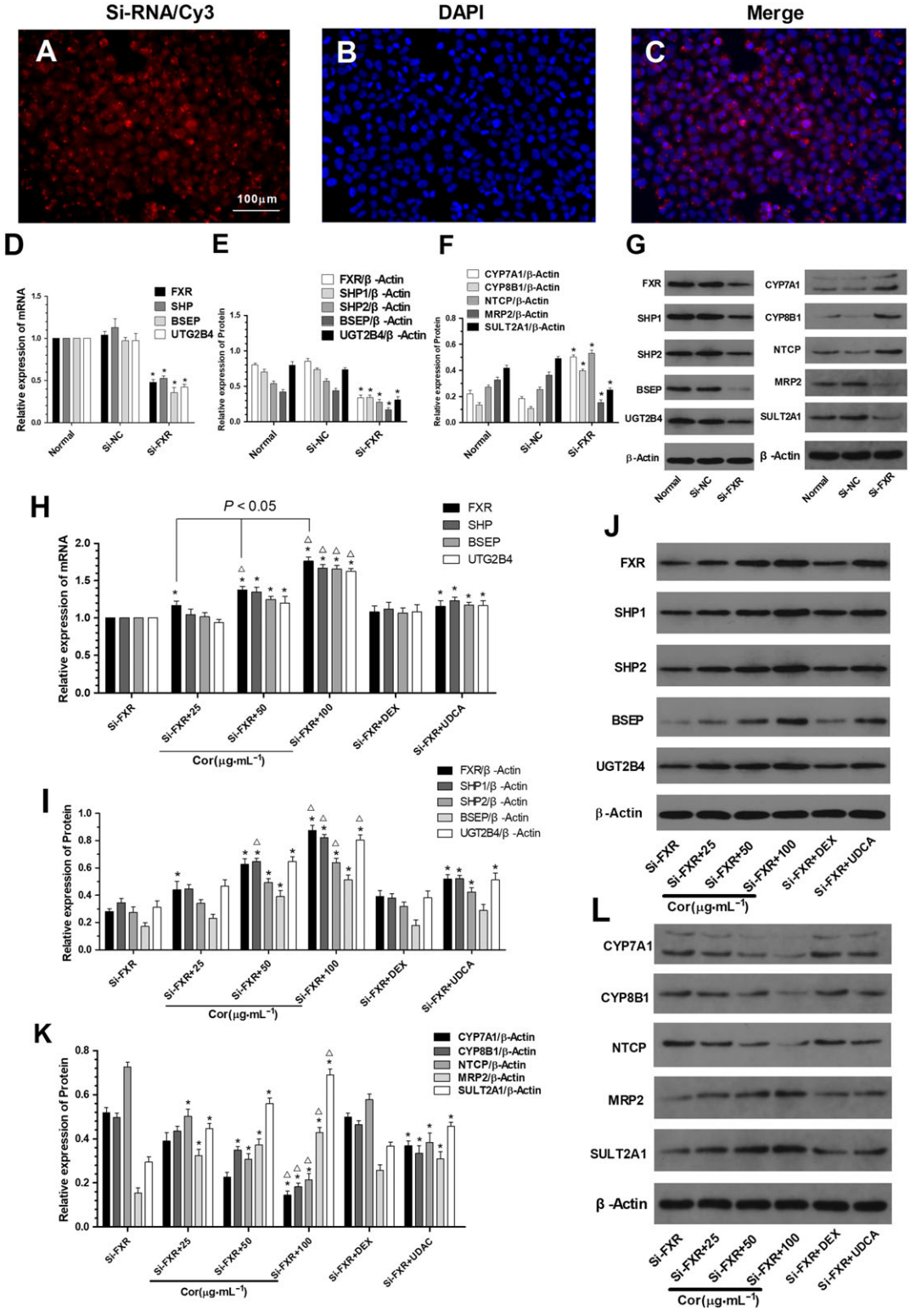

Figure 5

Down-regulation of FXR in LO2 cells via siRNA-FXR. The siRNA interfered with the FXR in LO2 cells for 24 h to down-regulate the expression of FXR, and then the cells were treated with different drugs for 24 h. (A–C) The fluorescent molecules Cy3 were observed with a fluorescence microscope after siRNA was introduced into LO2 cells for 24 h compared with the same perspective of ordinary light. (D, H) The mRNA levels of FXR SHP, BSEP and UGT2B4 were detected by RT-PCR. (E–G, I–L) The protein levels of FXR, SHP1, SHP2, BSEP, UGT2B4, MRP2, SULT2A1, CYP7A1, CYP8B1 and NTCP were detected by Western blotting. Data were shown as the mean ± SD. $n = 5$. (*$P < 0.05$ compared to the Si-FXR group; △$P < 0.05$ compared to the UDCA group). SiRNA-NC: siRNA negative control group.

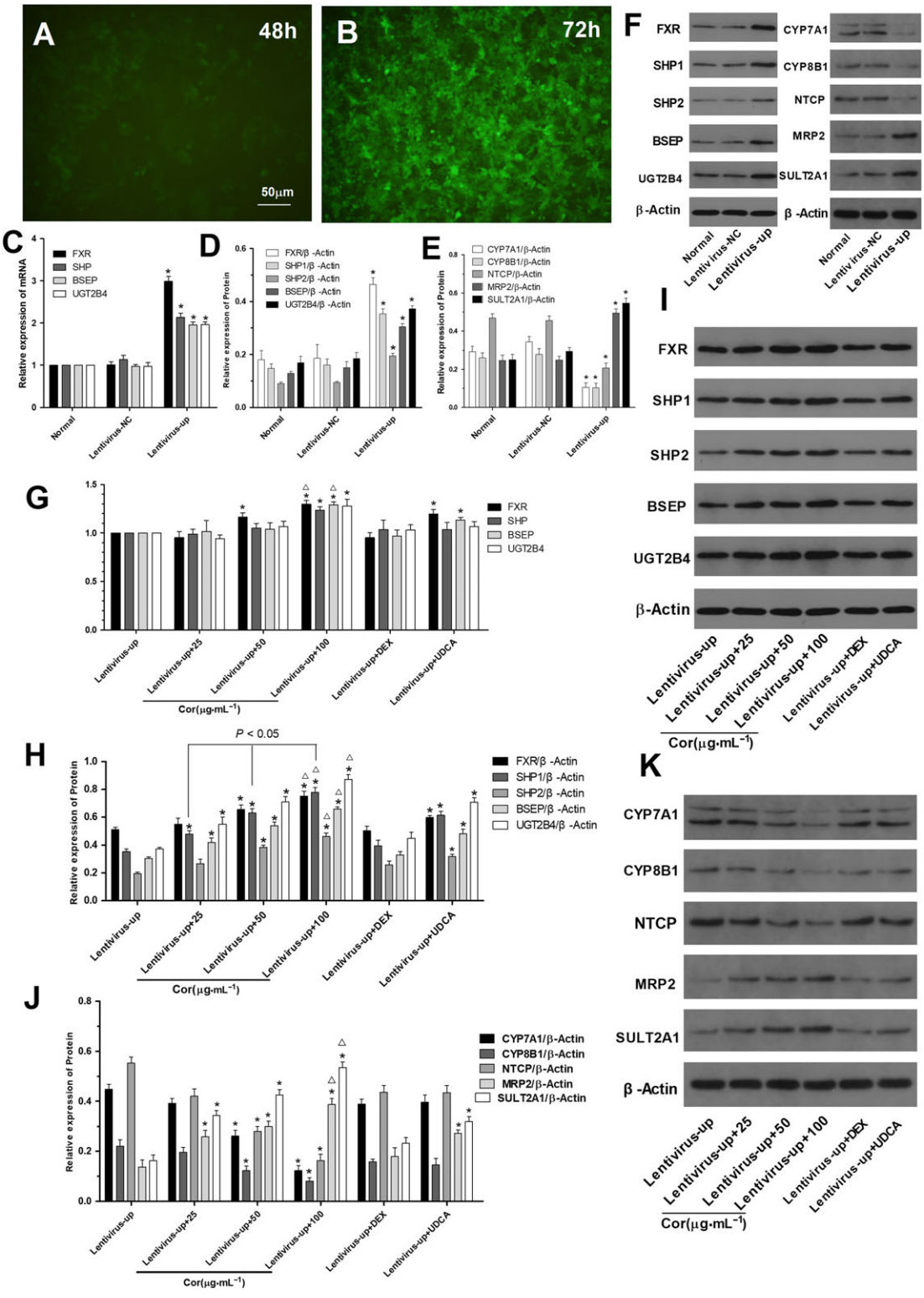

Figure 6

Up-regulation of FXR in LO2 cells via the lentiviral vector. The lentiviral vector interfered with LO2 cells for 72 h to mediate FXR overexpression. Then, the cells were treated with different drugs for 24 h. (A, B) The expression of GFP was observed with a fluorescence microscope after the lentivirus was introduced into LO2 cells for 48 and 72 h. (C, G) The mRNA levels of FXR SHP, BSEP and UGT2B4 were detected by RT-PCR. (D–F, H–K) The protein levels of FXR, SHP1, SHP2, BSEP, UGT2B4, NTCP, MRP2, SULT2A1, CYP7A1 and CYP8B1 were detected by Western blotting. Data are shown as the mean ± SD. $n = 5$. (*$P < 0.05$ compared to the Normal group/Lentivirus-treated group; △$P < 0.05$ compared to the UDCA group). Lentivirus-NC: lentivirus negative control group.

the corilagin and UDCA groups showed significantly elevated protein expression levels of FXR, SHP1, SHP2, UGT2B4, BSEP, MRP2 and SULT2A1 and reduced protein expression levels of CYP7A1, CYP8B1 and NTCP. In addition, the FXR, SHP1, SHP2, BSEP, UGT2B4, MRP2, SULT2A1, CYP7A1, CYP8B1 and NTCP protein levels in the 100 $\mu g \cdot mL^{-1}$ corilagin groups were significantly different (enhanced or reduced) than those in the UDCA group. Additionally, the activating effect of the FXR protein increased as the concentration of corilagin increased (Figure 6H–K).

Effects of corilagin on FXR and downstream molecules in rat primary hepatocytes

We used rat primary hepatocytes to investigate the effect of corilagin on cholestasis. To verify whether the isolated cells were rat primary hepatocytes, an immunofluorescence method was used to detect CK-18 protein in hepatocytes. The green fluorescence molecule Dylight 488 in primary hepatocytes was observed under a fluorescence microscope (Figure 7A–C). After corilagin treatment, compared with the untreated cells, the corilagin group showed significantly elevated mRNA expression of FXR, SHP, UGT2B4 and BSEP, while the mRNA expression of SHP and BSEP in the UDCA group was also increased. More importantly, the increases in the mRNA levels of SHP and BSEP in the 100 $\mu g \cdot mL^{-1}$ corilagin group were more significant than those in the UDCA groups (Figure 7D). The protein expression levels of FXR, SHP1, SHP2, UGT2B4, BSEP, MRP2 and SULT2A1 were also significantly increased. Furthermore, CYP7A1, CYP8B1 and NTCP were decreased in the corilagin groups compared with the normal group, and there were no obvious increases in protein expression in the DEX and UDCA groups (Figure 7E, F). The primary hepatocyte experimental results were consistent with those of the LO2 liver cell line, as the FXR-associated pathways were markedly up-regulated in the 50 and 100 $\mu g \cdot mL^{-1}$ corilagin groups *in vitro*.

Effect of corilagin on serum biochemical indicator

As shown in Table 3, compared with the model group, the corilagin-treated groups showed significant decreases in ALT, AST, TBIL, DBIL, ALP, GGT and TBA levels. Corilagin (20 $mg \cdot kg^{-1}$) and corilagin (40 $mg \cdot kg^{-1}$) induced similar effects as UDCA on ALT. Corilagin (40 $mg \cdot kg^{-1}$) exhibited the greatest effects on AST, ALP and DBIL, but they were lower than those induced by UDCA. Corilagin (40 $mg \cdot kg^{-1}$, 20 $mg \cdot kg^{-1}$) had notable effects on TBIL ($n = 5$; $P < 0.05$), and UDCA induced a similar effect on TBIL levels as corilagin (10 $mg \cdot kg^{-1}$). Corilagin (10, 20 and 40 $mg \cdot kg^{-1}$) significantly influenced GGT, and this effect of corilagin (40 $mg \cdot kg^{-1}$) was more than that of UDCA.

Effects of corilagin on liver morphology as assessed using HE staining

As shown in Figure 8, the hepatic tissue in the normal group showed a regular arrangement of hepatic lobules and cells, and intact epithelial cells from the bile duct could also be observed. Compared with the normal group, the model group showed typical pathological changes, including significant swelling of hepatic cells, swelling of cytoplasm, disorganized nuclei and strongly stained nucleoli. Moreover, in the model group, many punctiform or focused necrotic zones were observed in the hepatic tissue, and a proliferation of bile duct epithelial cells and Kupffer's cells was also observed. In addition, the bile duct showed a narrower canal, a bile thrombus and necrotic cells. In the corilagin groups, the pathological changes were less pronounced than those in the model group, and the morphological changes in the UDCA group were similar to those observed in the corilagin (20 $mg \cdot kg^{-1}$) group. However, the pathological impairments in the DEX group appeared to be more severe in hepatic tissue.

Effect of corilagin on BSEP protein expression in liver tissues as examined by immunohistochemistry

As shown in Figure 8, the rate of BSEP-positive staining in the cytoplasm in specimens from the model group significantly decreased compared with that in the normal group. However, after corilagin treatment, the rate was notably increased. The staining intensity in the UDCA group was higher than that in the model group. Compared with the UDCA group, the corilagin (20 $mg \cdot kg^{-1}$) and corilagin (40 $mg \cdot kg^{-1}$) groups had markedly higher positive staining, while the positive staining in the DEX group showed no marked differences compared with the model group.

Effects of corilagin on FXR pathways in a rat model of cholestatic hepatitis

Compared with the normal group, the model group showed significantly decreased mRNA levels of FXR, SHP, BSEP and UGT2B4. The mRNA expression of FXR, SHP, BSEP and UGT2B4 in the corilagin and UDCA groups and the mRNA expression of SHP in the DEX group were significantly altered compared with the model group. In addition, the SHP mRNA level in the 20 and 40 $mg \cdot kg^{-1}$ corilagin groups and the UDCA group were significantly higher than that in the DEX group. The FXR, SHP, BSEP and UGT2B4 mRNA levels in the 40 $mg \cdot kg^{-1}$ corilagin group were greater than those in the UDCA group. Furthermore, the activating effect of FXR mRNA increased as the concentration of corilagin increased (Figure 9B). Compared with the normal group, the model group exhibited significantly decreased protein expression levels of FXR, SHP1, SHP2, UGT2B4 and BSEP. However, compared with the model group, the corilagin and UDCA groups showed significantly elevated protein expression levels of FXR, SHP1, SHP2, UGT2B4, BSEP, MRP2 and SULT2A1 as well as reduced protein expression levels of CYP7A1, CYP8B1 and NTCP. The protein expression levels of SHP2, UGT2B4, BSEP, CYP8B1 and SULT2A1 in the DEX group were also significantly elevated or reduced (Figure 9C, D). Although UDCA exerted a positive effect on the protein expression of FXR, SHP1, SHP2, BSEP, UGT2B4, DEX, CYP8A1 and CYP8B1, and although DEX induced a positive effect on the protein expression of SHP2, BSEP, UGT2B4, CYP8B1 and SULT2A1, these effects were more marked in the corilagin (40 $mg \cdot kg^{-1}$) group than in the UDCA and DEX groups.

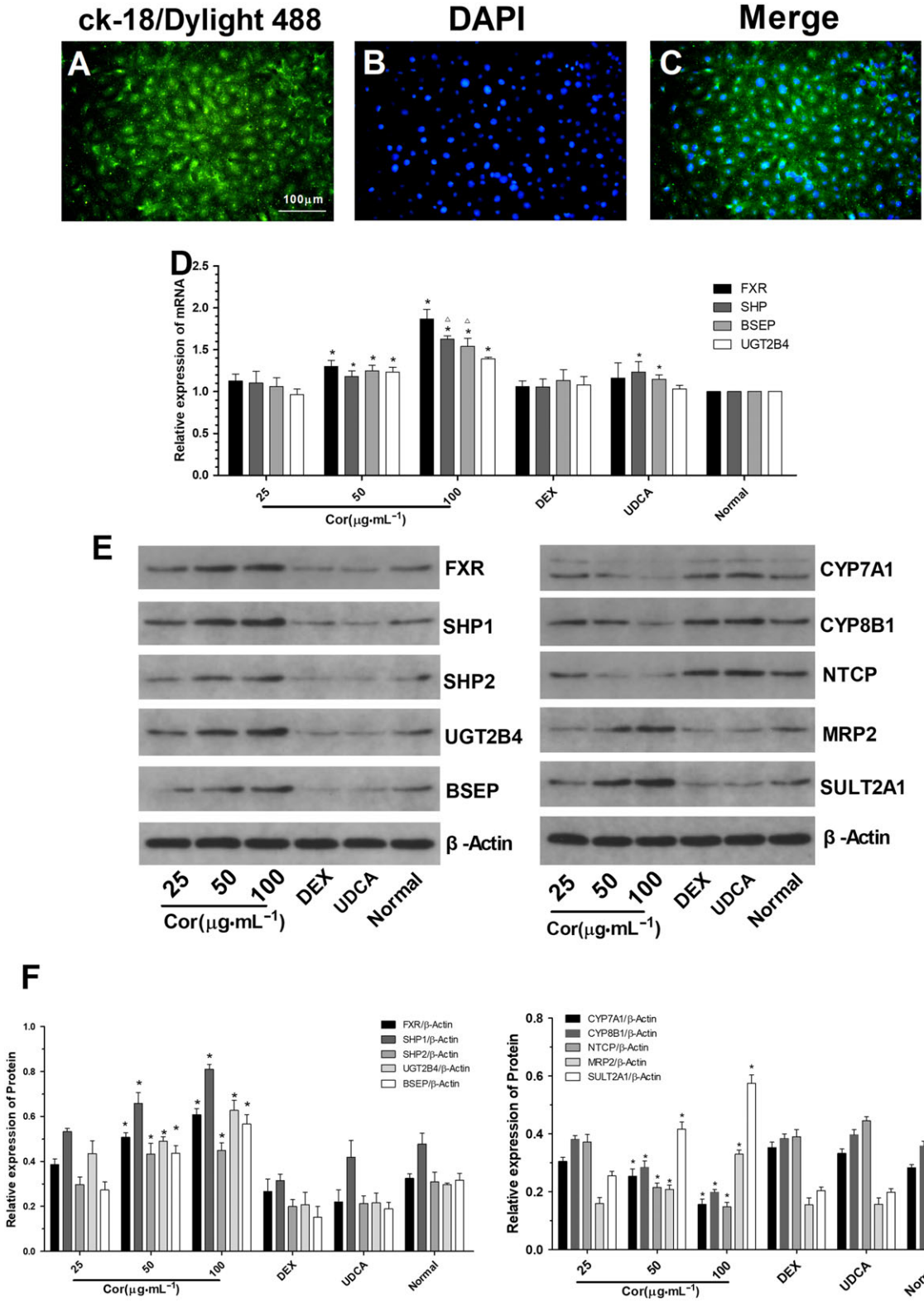

Figure 7

Effects of corilagin on FXR and downstream effectors in rat primary hepatocytes. Immunofluorescence was used to detect CK-18 protein in hepatocytes, and the green fluorescence molecule Dylight 488 in primary hepatocytes was observed under a fluorescence microscope (A–C). The mRNA levels of FXR, SHP, BSEP and UGT2B4 were detected by RT-PCR. (D) The protein levels of FXR, SHP1, SHP2, BSEP, UGT2B4, MRP2, SULT2A1, CYP7A1, CYP8B1 and NTCP were detected by Western blotting. Data are shown as the mean ± SD. $n = 5$. (*$P < 0.05$ compared to the Normal group).

Table 3

Effect of corilagin on liver function tests

Group	ALT (U.L^{-1})	AST (U.L^{-1})	TBIL (μM)	DBIL (μM)	ALP (U.L^{-1})	γ-GGT (U.L^{-1})	TBA (μM)
Corilagin (10 mg·kg^{-1})	785.8 ± 56.4$^{*,\#,\&,※}$	1243.8 ± 120.6$^{*,※}$	70.7 ± 12.9$^{*,\#}$	55.2 ± 12.1$^{*,\#}$	802.0 ± 97.6$^{*,\#,\&}$	5.4 ± 1.1$^{*,\#}$	156.6 ± 18.3$^{*,\#,※}$
Corilagin (20 mg·kg^{-1})	739.6 ± 104.1$^{*,\#,※}$	996.6 ± 216.6$^{*,\#,※}$	57.4 ± 6.8$^{*,\#}$	47.4 ± 9.3$^{*,\#}$	507.8 ± 94.9$^{*,\#,※}$	4.8 ± 0.8$^{*,\#}$	149.0 ± 32.3$^{*,\#,※}$
Corilagin (40 mg·kg^{-1})	439.6 ± 172.1$^{*,\#,※}$	764.2 ± 119.8$^{*,\#,\&,※}$	55.7 ± 7.6$^{*,\#}$	37.4 ± 10.1$^{*,\#,\&,※}$	353.0 ± 58.3$^{*,\#,\&,※}$	3.4 ± 0.5$^{*,\#,※}$	117.2 ± 27.2$^{*,\#,\&,※}$
Dexamethasone	1372.4 ± 226.3$^{*,\&}$	1572.2 ± 227.0$^{*,\&}$	72.5 ± 14.5*	60.3 ± 9.6*	833.0 ± 49.7$^{*,\#,\&}$	6.6 ± 1.5$^{*,\#,※}$	235.6 ± 18.8*
UDCA	527.2 ± 217.1$^{*,\#,※}$	1076. ± 231.9$^{*,\#,※}$	69.2 ± 16.0$^{*,\#}$	58.8 ± 10.3$^{*,\#}$	596.4 ± 99.7$^{*,\#,※}$	4.0 ± 1.2$^{*,\#}$	136.6 ± 43.8$^{*,\#,※}$
Model	888.6 ± 41.5*	1471.2 ± 254.2*	92.3 ± 13.4*	76.4 ± 13.6*	949.4 ± 70.8*	10.8 ± 2.3*	199.8 ± 37.6*
Normal	51.6 ± 22.7	140.4 ± 30.3	1.6 ± 0.5	0.9 ± 0.2	272.6 ± 45.8	3.4 ± 0.5	15.8 ± 6.1

Data were shown as mean ± SD. $n = 5$.

*$P < 0.05$ versus Normal group;

#$P < 0.05$ versus Model group;

&$P < 0.05$ versus UDCA group;

※$P < 0.05$ versus Dexamethasone group.

Discussion

Bile acids are produced in the liver by the oxidation of cholesterol through a series of reactions carried out by various cytochromes P450 enzymes (CYP) and CYP7A1, the latter of which is generally considered the rate-limiting enzyme that initiates bile acid synthesis (Gonzalez *et al.,* 2016). The physiological concentration of BAs can regulate liver regeneration (Huang *et al.,* 2006), energy expenditure (Watanabe *et al.,* 2006), triglyceride levels (Watanabe *et al.,* 2004) and glucose homeostasis (Thomas *et al.,* 2009). However, cholestasis patients who have excessive BAs can suffer from oxidative stress, hepatocyte death and mitochondrial abnormalities, all of which can ultimately induce liver damage.

Therefore, early effective interventions to control the development of cholestasis are particularly important. UDCA is currently the only Food and Drug Administration (FDA)-approved drug to treat primary biliary cirrhosis (PBC), but its efficacy is limited to early stages of the disease (Corpechot *et al.,* 2011). UDCA has been shown to promote the excretion of endogenous cholic acid, change the composition of BAs, increase the proportion of hydrophilic BAs, protect liver cells and bile duct cells from toxic BAs and inhibit liver cell apoptosis (Beuers, 2006). However, depending on age and sex, nearly 30–50% of patients are biochemical non-responders are, therefore, still at risk of disease progression and poor survival (Kuiper *et al.,* 2009; Corpechot *et al.,* 2008). Other medications such as S-adenosyl-L-methionine suffer from a lack of randomized controlled trials that have validated their efficacy (Lu and Mato, 2012). Although glucocorticoids have a limited effect on cholestasis, long-term use of glucocorticoids can cause many adverse effects, including weight gain, hyperglycaemia, osteoporosis, cataracts and increased risk of opportunistic infections (Purohit and Cappell, 2015).

Therefore, it is critical to find new drugs with fewer side effects that are reliable at treating cholestasis. Although the mechanisms of aberrant BA retention via synthesis, detoxification and transport are complicated, the multistep feedback loop that regulates BA involves the nuclear receptors FXR and SHP and culminates in the repression of CYP7A1 expression (Anakk *et al.,* 2011). FXR is a member of the nuclear receptor superfamily and is largely expressed in the liver (Fiorucci and Distrutti, 2015). Additionally, FXR has been recognized as a therapeutic target in cholestasis and has been confirmed as a key participant in the maintenance of BAs by regulating target genes related to the metabolism of BAs – particularly its synthesis, detoxification and transportation (Sepe *et al.,* 2015; Mazuy *et al.,* 2015). The role of FXR in cholestasis is as follows (Figure 10). In the BA detoxification pathway, UGT2B4 and SULT2A1 are influenced by FXR and transduce a detoxification signal that overrides other signals (Zollner and Trauner, 2009). In the BA transportation process, BSEP, NTCP and MRP2 are involved in the transfer of bile components after they are activated by FXR. BSEP, NTCP and MRP2 are abundantly expressed at the capillary bile duct membrane of hepatocytes and function as rate-limiting enzymes, making them key proteins in bile transportation and excretion. FXR upregulates the expression of BSEP by binding to its DNA response element and assisting BA transport from hepatocytes to the biliary duct (Gonzalez, 2012). During the

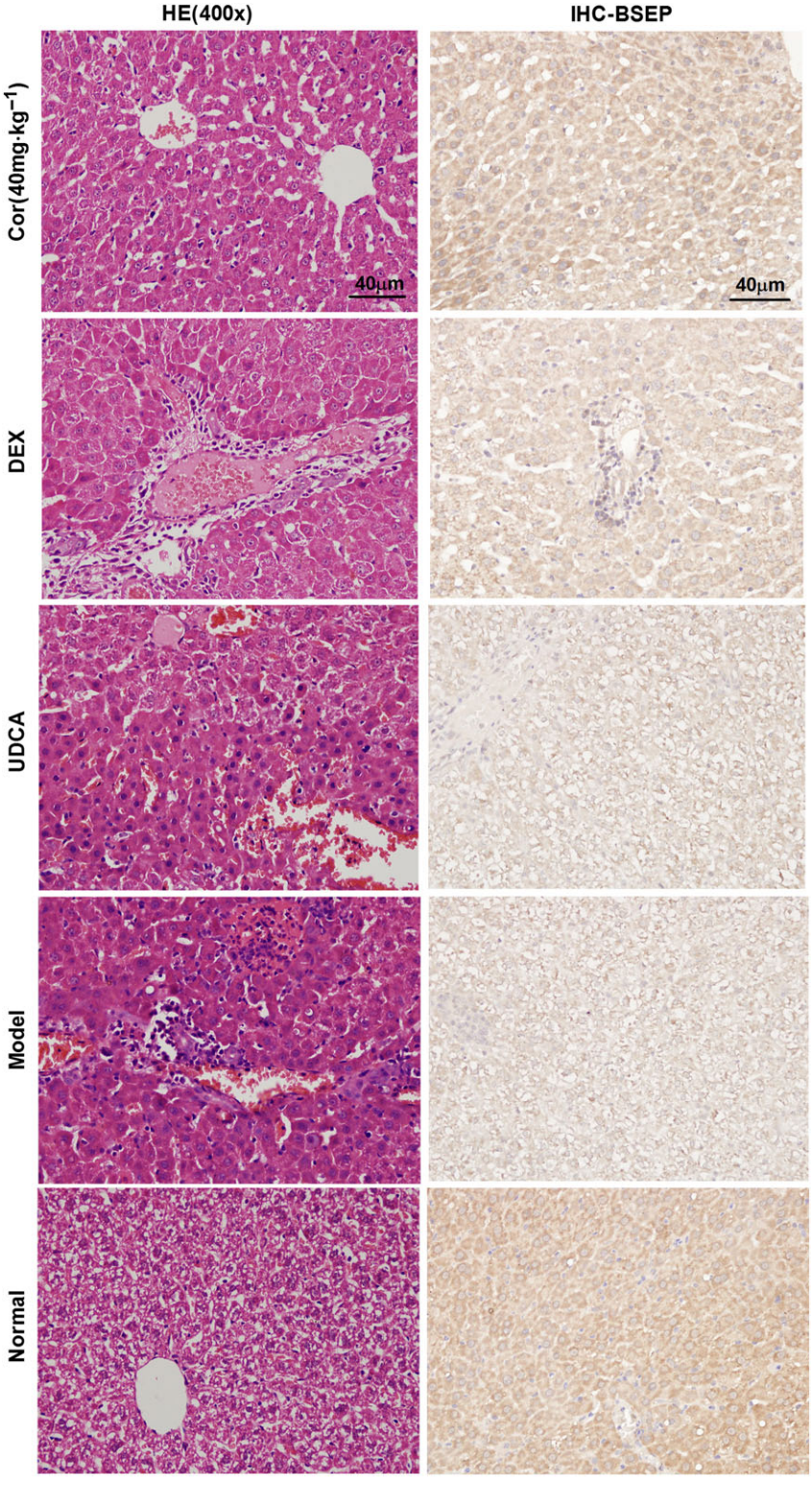

Figure 8

Effect of corilagin, in a rat model of cholestasis, on the pathological manifestation of choleostasis in hepatic tissue, as observed by HE staining in 400× magnification. The effect of corilagin on BSEP expression was examined with IHC.

process of BA synthesis, FXR either directly or indirectly represses the transcription of CYP7A1 and CYP8B1, which is required for the synthesis of BAs, by either mediating the expression of SHP or suppressing the degradation of SHP. This results in inhibition of BA synthesis, and the FXR can increase the content of bile phospholipids via small

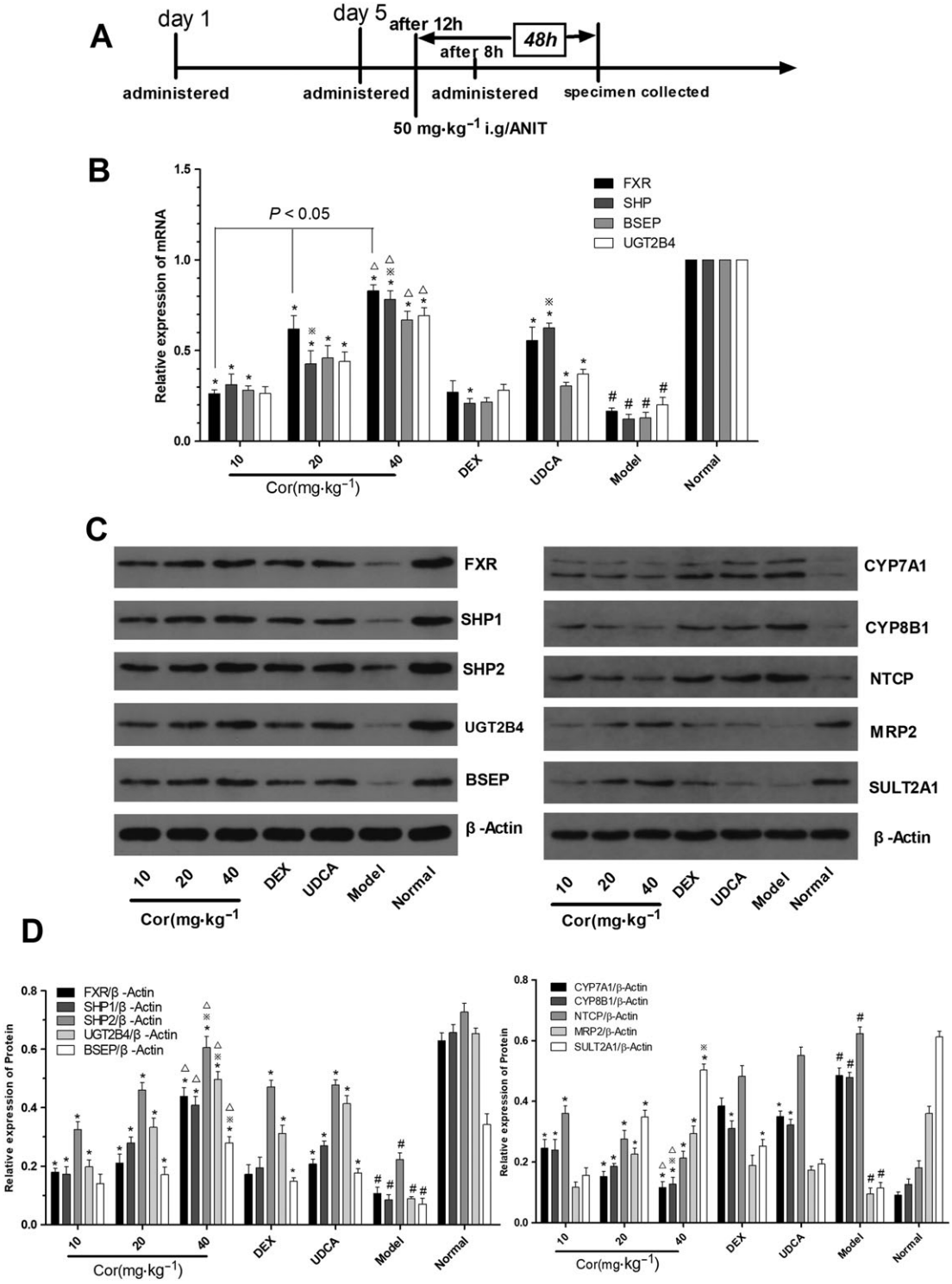

Figure 9

Effect of corilagin on the levels of FXR, SHP, BSEP, UGT2B4, MRP2, NTCP, SULT2A1, CYP7A1 and CYP8B1 in ANIT-treated rats. (A) The administration time point: drugs were administered to the rats in the respective groups for 4 days. On the fifth day, we administered drugs to the rats. After 12 h, all groups except the normal group were intragastrically administered ANIT (50 mg·kg^{-1}). After an 8 h interval of ANIT treatment, the rats were administered the respective drug or control agent. Forty eight hours after the ANIT treatment the rats in each group were killed for taking specimens. (B) The mRNA levels of FXR, SHP, BSEP and UGT2B4 were measured by real-time PCR. (C, D) The protein levels of FXR, SHP1, SHP2, BSEP, UGT2B4, MRP2, SULT2A1, NTCP, CYP7A1 and CYP8B1 were detected by Western blotting. Data are expressed as the mean ± SD. $n = 5$. (*$P < 0.05$ compared to the Model group; #$P < 0.05$ compared to the Normal group; △$P < 0.05$ compared to the UDCA group; ※$P < 0.05$ compared to the DEX group).

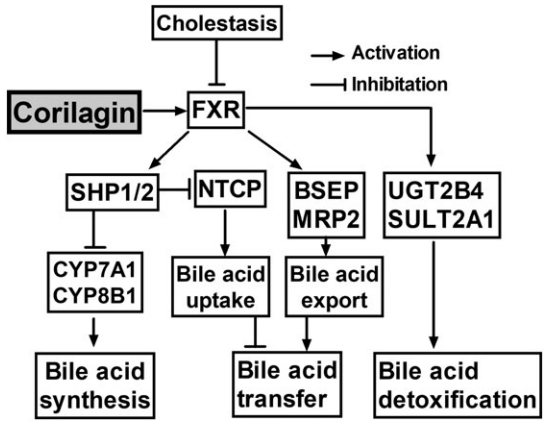

Figure 10

FXR plays an important role in the synthesis, detoxification and transport of bile acids. Corilagin was effective in activating the FXR signalling pathways to alleviate cholestasis.

heterodimer partner 1/2 (SHP1/2) and inhibit liver fibrosis via SHP1/2 and PPARγ (Wagner *et al.,* 2009).

For the *in vitro* experiment, the mRNA and protein expression levels of FXR, SHP, UGT2B4, BSEP, MRP2, SULT2A1, CYP7A1, CYP8B1 and NTCP were significantly elevated or reduced in the corilagin group compared with those in the normal group. Then, LO2 cells were treated with guggulsterones or si-FXR to inhibit FXR. Compared with the guggulsterones or si-FXR group, the corilagin groups showed significantly elevated mRNA and protein expression levels of FXR, SHP, UGT2B4, BSEP, MRP2 and SULT2A1 and reduced protein expression levels of CYP7A1, CYP8B1 and NTCP. Furthermore, to confirm the efficacy of corilagin, we treated LO2 cells with either GW4064 or lentivirus to enhance FXR activity. Compared with the GW4064 or lentivirus-treated group, the corilagin groups showed significantly elevated mRNA and protein expression of FXR, SHP, UGT2B4 BSEP, MRP2 and SULT2A1, together with reduced protein expression levels of CYP7A1, CYP8B1 and NTCP. In the *in vivo* experiments, FXR signalling pathways were activated in rats with ANIT-induced cholestasis. After establishing the cholestasis model and providing treatments, the serum TBIL, DBIL, TBA, ALP, GGT, ALT and AST levels as well as pathological changes in the liver were monitored. Corilagin at a dose of 20 mg·kg^{-1} in rats exerts remarkable effects on TBA and can also improve liver functions, related enzyme dysregulation and the jaundice index. Based on biochemical and pathological observations, ANIT-induced intrahepatic cholestasis and liver damage were observed in the model cholestasis group, thus proving successful establishment of this animal model. Regarding the hepatic pathology, the livers from rats subjected to ANIT administration exhibited typical damage, such as infiltration of neutrophils, necrosis of hepatocytes, proliferation of inflammatory cells and epithelial cells in the bile duct and formation of bile thrombus. Corilagin improved these acute hepatic impairments. The expression levels of FXR, SHP1, SHP2, BSEP, UGT2B4, MRP2, SULT2A1, CYP7A1, CYP8B1 and NTCP were significantly decreased or increased in the model group. After treatment with corilagin, the FXR pathways were markedly activated, and the expression levels of FXR, SHP, BSEP, UGT2B4, MRP2, SULT2A1, CYP7A1, CYP8B1 and NTCP were promoted or inhibited to varying degrees.

In our experiments, several details deserve further attention. Firstly, one concentration cannot reflect a dose-dependent effect and, therefore, we chose three corilagin concentrations. Cells treated with siRNA-FXR + corilagin 100 μg·mL^{-1} had higher levels of FXR than normal cells (seen in Figure 5), and siRNA-FXR + UDCA treatment increased FXR expression, while UDCA alone did not affect FXR in the normal group (based on the literature and the data shown in Figure 2). In LO2 cells treated with siRNA with lower levels of FXR, the effect of the drug on promoting FXR was notable, and corilagin 100 μg·mL^{-1} promoted FXR in normal LO2 cells. UDCA had no effects on normal LO2 cells, but whether it exerts effects on distressed cells remains unknown. However, from the subsequent results, regardless of treatment with guggulsterones, GW4064, siRNA or lentivirus, UDCA had notable effects. Furthermore, although guggulsterones and siRNA as well as GW4064 and the lentivirus vector exerted similar effects on FXR gene expression to either inhibit or promote FXR by 50%, respectively, the mechanisms of action are completely different. The siRNA and lentiviral vectors target the specific gene, whereas the use of a chemical antagonist (guggulsterones) or agonist (GW4064) can affect FXR-associated pathways in multiple manners, the exact mechanisms of which are unknown. Therefore, we chose both chemical and biological approaches to interfere with the expression of FXR. Moreover, Fxr-knockout (Fxr−/−) animals have excessive levels of BAs, cholesterol and triglycerides. In addition, the FXR-associated pathways in human cholestasis have been shown to be suppressed, although only a few studies have knocked out FXR to observe the effect of the FXR gene in humans. Therefore, the LO2 cells were treated with guggulsterones or siRNA to down-regulate FXR expression to simulate low FXR expression. In contrast, the FXR agonist GW4064 reduced cholestasis and has been approved for the treatment of PBC and NASH. However, to observe whether corilagin continues to promote the FXR signalling pathway under conditions of high FXR expression, we chose GW4064 and a lentiviral vector to up-regulate FXR in cells. Additionally, to maintain stable blood drug concentrations, we pretreated cells with the respective compounds. Cholestasis in an animal model has a rapid onset, and the most serious damage occurs at 48 h. Drugs administered after induction of the cholestasis in this model would miss the opportunity to exert effects during the acute stage of disease. However, in clinical practice, cholestasis normally requires an extended treatment regime, and the efficacy would be obvious after the medication arrived at a stable blood drug concentration. Therefore, we administered medication prior to inducing the model in order to achieve a stable blood drug concentration and to reflect the efficacy of corilagin for treating cholestasis. As a result, corilagin was shown to be an effective therapy. However, further work is necessary before progressing this drug to clinical trials.

In summary, we investigated the efficacy of corilagin in activating the FXR signalling pathway to alleviate cholestasis *in vitro* and *in vivo*, which could specifically affect the synthesis, detoxification and transport of bile acids. More importantly, we demonstrated that corilagin could regulate the

key target molecule FXR, which has been verified as a viable therapeutic target for the development of drugs to treat intrahepatic cholestasis. This study not only focused on the reliable curative effects but also opened up a new area of gene targeting therapy, providing a new avenue for clinical research and treatment and forming the foundation for future precision medicine for intrahepatic cholestasis. Further studies on the mechanism of by which corilagin alleviates cholestasis may help identify new methods to prevent and treat intrahepatic cholestasis.

Acknowledgements

This study was supported by the National Natural Science Foundation of China (81371840 and 81600373), the Hubei Province Health and Family Planning Scientific Research Project (WJ2017Q021), the Hubei Provincial Natural Science Foundation of China (2017CFB471), the Fundamental Research Funds for the Central Universities (2017KFYXJJ238) and Shandong Provincial Natural Science Foundation of China (2016ZRB14450).

The study was reviewed and approved by the Research Ethics Committee of Tongji Medical College, Huazhong University of Science and Technology [(2015) IACUC Number: 513].

Author contributions

L.Z. takes responsibility for the integrity of the work as a whole, from inception to publication. F.Y. conceived and designed the experiments. Y.W., Z.-L.C., J.X. and L.L. performed the experiments. G.L. analysed the data. Z.-L.C., F.J., L.L., X.Z., Q.M., X.C. and H.-R.L. contributed reagents, materials or analysis tools. Y.W., L.G. and Z.-L.C. wrote the paper. L.Z. edited the article. All authors approved the final version of the manuscript.

Conflict of interest

The authors declare no conflicts of interest.

Declaration of transparency and scientific rigour

This Declaration acknowledges that this paper adheres to the principles for transparent reporting and scientific rigour of preclinical research recommended by funding agencies, publishers and other organisations engaged with supporting research.

References

Alexander SPH, Cidlowski JA, Kelly E, Marrion NV, Peters JA, Faccenda E *et al*. (2017a). The Concise Guide to PHARMACOLOGY 2017/18: Nuclear hormone receptors. Br J Pharmacol 174: S208–S224.

Alexander SPH, Fabbro D, Kelly E, Marrion NV, Peters JA, Faccenda E *et al*. (2017b). The Concise Guide to PHARMACOLOGY 2017/18: Enzymes. Br J Pharmacol 174: S272–S359.

Alexander SPH, Kelly E, Marrion NV, Peters JA, Faccenda E, Harding SD *et al*. (2017c). The Concise Guide to PHARMACOLOGY 2017/18: Transporters. Br J Pharmacol 174: S360–S446.

Anakk S, Watanabe M, Ochsner SA, McKenna NJ, Finegold MJ, Moore DD (2011). Combined deletion of Fxr and Shp in mice induces Cyp17a1 and results in juvenile onset cholestasis. J Clin Invest 121: 86–95.

Banaudha K, Orenstein JM, Korolnek T, St Laurent GC 3rd, Wakita T, Kumar A (2010). Primary hepatocyte culture supports hepatitis C virus replication: a model for infection-associated hepatocarcinogenesis. Hepatology 51: 1922–1932.

Beuers U (2006). Drug insight: mechanisms and sites of action of ursodeoxycholic acid in cholestasis. Nat Clin Pract Gastroenterol Hepatol 3: 318–328.

Beuers U, Trauner M, Jansen P, Poupon R (2015). New paradigms in the treatment of hepatic cholestasis: from UDCA to FXR, PXR and beyond. J Hepatol 62: S25–S37.

Chen P, Zeng H, Wang Y, Fan X, Xu C, Deng R *et al*. (2014). Low dose of oleanolic acid protects against lithocholic acid-induced cholestasis in mice: potential involvement of nuclear factor-E2-related factor 2-mediated upregulation of multidrug resistance-associated proteins. Drug Metab Dispos 42: 844–852.

Chen Z, Zhu Y, Zhao Y, Ma X, Niu M, Wang J *et al*. (2016). Serum metabolomic profiling in a rat model reveals protective function of paeoniflorin against ANIT induced cholestasis. Phytother Res 30: 654–662.

Cheng JT, Lin TC, Hsu FL (1995). Antihypertensive effect of Corilagin in the rat. Can J Physiol Pharmacol 73: 1425–1429.

Corpechot C, Abenavoli L, Rabahi N, Chrétien Y, Andréani T, Johanet C *et al*. (2008). Biochemical response to ursodeoxycholic acid and long-term prognosis in primary biliary cirrhosis. Hepatology 48: 871–877.

Corpechot C, Chazouilleres O, Poupon R (2011). Early primary biliary cirrhosis: biochemical response to treatment and prediction of longterm outcome. J Hepatol 55: 1361–1367.

Curtis MJ, Bond RA, Spina D, Ahluwalia A, Alexander SP, Giembycz MA *et al*. (2015). Experimental design and analysis and their reporting: new guidance for publication in BJP. Br J Pharmacol 172: 3461–3471.

Dang YP, Chen YF, Li YQ, Zhao L (2016). Developments of anticoagulants and new agents with anti-coagulant effects in Deep Vein Thrombosis. Mini Rev Med Chem 17: 1–13.

Ding L, Yang L, Wang Z, Huang W (2015b). Bile acid nuclear receptor FXR and digestive system diseases. Acta Pharm Sin B 5: 135–144.

Ding Y, Li G, Xiong LJ, Yin W, Liu J, Liu F *et al*. (2015a). Profiles of responses of immunological factors to different subtypes of Kawasaki disease. BMC Musculoskelet Disord 16: 315.

Ding Y, Xiong XL, Zhou LS, Yan SQ, Qin H, Li HR *et al*. (2016). Preliminary study on Emodin alleviating alpha-naphthylisothiocyanate-induced intrahepatic cholestasis by regulation of liver farnesoid X receptor pathway. Int J Immunopathol Pharmacol 29: 805–811.

Ding Y, Zhao L, Mei H, Huang ZH, Zhang SL (2006). Alterations of biliary biochemical constituents and cytokines in infantile hepatitis syndrome. World J Gastroenterol 12: 7038–7041.

Ding Y, Zhao L, Mei H, Zhang SL, Huang ZH, Duan YY *et al*. (2008). Exploration of Emodin to treat alpha-naphthylisothiocyanate-induced cholestatic hepatitis via anti-inflammatory pathway. Eur J Pharmaco 590: 377–386.

Du P, Ma Q, Zhu ZD, Li G, Wang Y, Li QQ *et al*. (2016). Mechanism of Corilagin interference with IL-13/STAT6 signaling pathways in hepatic alternative activation macrophages in schistosomiasis-induced liver fibrosis in mouse model. Eur J Pharmacol 793: 119–126.

Duan W, Yu Y, Zhang L (2005). Antiatherogenic effects of Phyllanthus emblica associated with Corilagin and its analogue. Yakugaku Zasshi 125: 587–591.

Fiorucci S, Distrutti E (2015). Bile acid-activated receptors, intestinal microbiota, and the treatment of metabolic disorders. Trends Mol Med 21: 702–714.

Gambari R, Borgatti M, Lampronti I, Fabbri E, Brognara E, Bianchi N *et al*. (2012). Corilagin is a potent inhibitor of NF-kappa B activity and downregulates TNF-alpha induced expression of IL-8 gene in cystic fibrosis IB3-1 cells. Int Immunopharmacol 13: 308–315.

Gonzalez FJ (2012). Nuclear receptor control of enterohepatic circulation. Compr Physiol 2: 2811–2828.

Gonzalez FJ, Jiang C, Patterson AD (2016). An intestinal microbiota-farnesoid X receptor axis modulates metabolic disease. Gastroenterology 151: 845–859.

Guo YJ, Luo T, Wu F, Liu H, Li HR, Mei YW *et al*. (2015). Corilagin protects against HSV1 encephalitis through inhibiting the TLR2 signaling pathways *in vivo* and *in vitro*. Mol Neurobiol 52: 1547–1560.

Guo YJ, Zhao L, Li XF, Mei YW, Zhang SL, Tao JY *et al*. (2010). Effect of Corilagin on anti-inflammation in HSV-1 encephalitis and HSV-1 infected microglias. Eur J Pharmacol 635: 79–86.

Huang W, Ma K, Zhang J, Qatanani M, Cuvillier J, Liu J *et al*. (2006). Nuclear receptor-dependent bile acid signaling is required for normal liver regeneration. Science 312: 233–236.

Huang YF, Zhang SL, Jin F, Cheng D, Zhou YP, Li HR *et al*. (2013). Activity of Corilagin on postparasiticide liver fibrosis in schistosomiasis animal model. Int J Immunopathol Pharmacol 26: 85–92.

Jia L, Jin H, Zhou J, Chen L, Lu Y, Ming Y *et al*. (2013). A potential anti-tumor herbalmedicine, Corilagin, inhibits ovarian cancer cell growth through blocking the TGF-β signaling pathways. BMC Complement Altern Med 15: 33.

Jin F, Cheng D, Tao JY, Zhang SL, Pang R, Guo YJ *et al*. (2013). Anti-inflammatory and anti-oxidative effects of Corilagin in a rat model of acute cholestasis. BMC Gastroenterol 13: 79.

Jin F, Zhang R, Feng S, Yuan CT, Zhang RY, Han GK *et al*. (2015). Pathological features of transplanted tumor established by CD133 positive TJ905 glioblastoma stem-like cells. Cancer Cell Int 15: 60.

Kilkenny C, Browne W, Cuthill IC, Emerson M, Altman DG (2010). Animal research: reporting *in vivo* experiments: the ARRIVE guidelines. Br J Pharmacol 160: 1577–1579.

Klaunig JE, Goldblatt PJ, Hinton DE, LipskyMM CJ, Trump BF (1981). Mouse liver cell culture. I. Hepatocyte isolation. *In Vitro* 17: 913–925.

Kuiper EM, Hansen BE, de Vries RA, den Ouden-Muller JW, van Ditzhuijsen TJ, Haagsma EB *et al*. (2009). Improved prognosis of patients with primary biliary cirrhosis that have a biochemical response to ursodeoxycholic acid. Gastroenterology 136: 1281–1287.

Li HR, Li G, Li M, Zhang SL, Wang H, Luo T *et al*. (2016). Corilagin ameliorates schistosomiasis hepatic fibrosis through regulating IL-13 associated signal pathway *in vitro* and *in vivo*. Parasitology 143: 1629–1638.

Lu SC, Mato JM (2012). S-adenosylmethionine in liver health, injury, and cancer. Physiol Rev 92: 1515–1542.

Mazuy C, Helleboid A, Staels B, Lefebvre P (2015). Nuclear bile acid signaling through the farnesoid X receptor. Cell Mol Life Sci 72: 1631–1650.

McGrath JC, Lilley E (2015). Implementing guidelines on reporting research using animals (ARRIVE etc.): new requirements for publication in BJP. Br J Pharmacol 172: 3189–3193.

McKiernan PJ (2002). Neonatal cholestasis. Semin Neonatol 7: 153–165.

Neuschwander-Tetri BA, Loomba R, Sanyal AJ, Lavine JE, Van Natta ML, Abdelmalek MF *et al*. (2015). Farnesoid X nuclear receptor ligand obeticholic acid for non-cirrhotic, non-alcoholic steatohepatitis (FLINT): a multicentre, randomised, placebo-controlled trial. Lancet 385: 956–965.

Parés A (2015). Therapy of primary biliary cirrhosis: novel approaches for patients with suboptimal response to ursodeoxycholic acid. Dig Dis 33 (Suppl 2): 125–133.

Purohit T, Cappell MS (2015). Primary biliary cirrhosis: pathophysiology, clinical presentation and therapy. World J Hepatol 7: 926–941.

Schmittgen TD, Livak KJ (2008). Analyzing real-time PCR data by the comparative C (T) method. Nat Protoc 3: 1101–1108.

Seok S, Fu T, Choi SE, Li Y, Zhu R, Kumar S *et al*. (2014). Transcriptional regulation of autophagy by an FXR-CREB axis. Nature 516: 108–111.

Sepe V, Distrutti E, Fiorucci S, Zampella A (2015). Farnesoid X receptor modulators (2011–2014): a patent review. Expert Opin Ther Pat 25: 885–896.

Shen ZQ, Dong ZJ, Peng H, Liu JK (2003). Modulation of PAI-1 and tPA activity and thrombolytic effects of Corilagin. Planta Med 69: 1109–1112.

Shiota S, Shimizu M, Sugiyama J, Morita Y, Mizushima T, Tsuchiya T (2004). Mechanisms of action of Corilagin and tellimagrandin I that remarkably potentiate the activity of beta-lactams against methicillin-resistant Staphylococcus aureus. Microbiol Immunol 48: 67–73.

Southan C, Sharman JL, Benson HE, Faccenda E, Pawson AJ, Alexander SPH *et al*. (2016). The IUPHAR/BPS Guide to PHARMACOLOGY in 2016: towards curated quantitative interactions between 1300 protein targets and 6000 ligands. Nucl Acids Res 44: D1054–D1068.

Thomas C, Gioiello A, Noriega L, Strehle A, Oury J, Rizzo G *et al*. (2009). TGR5-mediated bile acid sensing controls glucose homeostasis. Cell Metab 10: 167–177.

Wagner M, Zollner G, Trauner M (2009). New molecular insights into the mechanisms of cholestasis. J Hepatol 51: 565–580.

Wang Y, Yang F, Xue J, Zhou X, Luo L, Ma Q *et al*. (2016). Anti-Schistosomiasis liver fibrosis effects of chlorogenic acid through IL-13/miR-21/Smad7 signaling interactions *in vivo* and *in vitro*. Antimicrob Agents Chemother 61 pii: e01347-16.

Watanabe M, Houten SM, Mataki C, Christoffolete MA, Kim BW, Sato H *et al*. (2006). Bile acids induce energy expenditure by promoting intracellular thyroid hormone activation. Nature 439: 484–489.

Watanabe M, Houten SM, Wang L, Moschetta A, Mangelsdorf DJ, Heyman RA *et al*. (2004). Bile acids lower triglyceride levels via a pathway involving FXR, SHP, and SREBP-1c. J Clin Invest 113: 1408–1418.

Yang F, Wang Y, Xue J, Ma Q, Zhang J, Chen YF *et al*. (2016). Effect of Corilagin on the miR-21/smad7/ERK signaling pathway in a schistosomiasis-induced hepatic fibrosis mouse model. Parasitol Int 65: 308–315.

Zhang XQ, Gu HM, Li XZ, Xu ZN, Chen YS, Li Y (2013). Anti-Helicobacter pylori compounds from the ethanol extracts of Geranium wilfordii. J Ethnopharmacol 147: 204–207.

Zhao C, Wang X, Cong Y, Deng Y, Xu Y, Chen A *et al*. (2014). Effects of bile acids and the bile acid receptor FXR agonist on the respiratory rhythm in the *in vitro* brainstemmedulla slice of neonatal sprague-dawley rats. PLoS ONE 9: e112212.

Zhao L, Zhang SL, Tao JY, Pang R, Jin F, Guo YJ *et al*. (2008). Preliminary exploration on anti-inflammatory mechanism of Corilagin (beta-1-O-galloyl-3,6-(R)-hexahydroxydiphenoyl-d-glucose) *in vitro*. Int Immunopharmacol 8: 1059–1064.

Zhou YP, Cheng D, Zhang SL, Li HR, Tang ZM, Xue J *et al*. (2016). Preliminary exploration on anti-fibrosis effect of kaempferol in mice with japonicum schistosoma infection. Eur J Inflamm 11: 161–168.

Zollner G, Trauner M (2009). Nuclear receptors as therapeutic targets in cholestatic liver diseases. Br J Pharmacol 156: 7–27.